Development and Evaluation of Mathematical Model to Simulate Thoracic Response to Impact in Lateral and Oblique Directions

Undergraduate Honors Thesis

Presented in Partial Fulfillment of the Requirements for

Graduation with Distinction

at The Ohio State University

By

Jason D. Miller

* * * * *

The Ohio State University

2010

Defense Committee:

Professor John Bolte, Advisor

Professor Manoj Srinivasan

Approved by

Advisor

Undergraduate Program in Mechanical Engineering

ABSTRACT

Various studies have sought to measure the mechanical response of the thorax of post mortem human specimens (PMHS) in order to predict injury associated with high speed impacts in the anterior and lateral (90 degrees from anterior) directions. Experimental data from these studies has been used to develop models to simulate thoracic response to impact, however these models have been limited in scope placing primary focus on impacts in the anterior direction. Accurate thoracic response models are critical in development of biofidelic crash test dummies and accurate crash safety standards. Initial research of the thoracic response assumed that the thorax exhibited a similar response to lateral (90 deg from anterior) and oblique (60 deg from anterior) impacts. The Ohio State University Injury Biomechanics Research Laboratory (IBRL) has been conducting experiments to understand the difference in thorax response as a result of alternate loading orientations. Data collected has shown a significant difference in impact response as loading is shifted from lateral to oblique angles. It is the hope that continued understanding of thoracic response from alternate angle points will lead to models that more accurately represent the thoracic response especially since impacts in an actual car crash will not necessarily solely cause impact in the anterior direction. The goal of this project is to develop a model that accurately depicts thoracic responses in both the lateral and oblique directions based on experimental data previously collected in the IBRL. Results show that initially there is not enough information to accurately

simulate the response of the thorax to impact separately for different impact speeds and orientations. More information characterizing the thoracic system is needed to perform such a simulation. However, comparison of simulated thoracic deflection compared with experimental thoracic deflection for low speed (2.5 m/s) impacts in both the lateral and oblique directions simultaneously showed that lateral and oblique internal mechanical response is more similar than initially understood.

ACKNOWLEDGMENTS

Significant credit must first and for most be given to Dr. John Bolte IV for providing significant technical support and motivation without which this project would have never been completed. The lessons learned while working closely with John will go a long way towards developing me into the professional engineer that I wish to be some day.

Additionally, thanks to Dr. Manoj Srinivasan for useful discussions about the optimization methods and model fitting.

The quality of this project was increased significantly through funding from the Engineering Experiment Station (EES) at The Ohio State University. Receiving tuition scholarship and monthly stipend through this organization allowed for more focused research which the benefits to this project are immeasurable.

TABLE OF CONTENTS

Page

LIST OF FIGURES

Figure Page

LIST OFTABLES

Table Page

CHAPTER 1

INTRODUCTION

1.1 Introduction

In the event of a traffic collision, the vehicle comes to an rapidly accelerated stop while the passenger continues in progress in the direction of the impact due to inertia of the body. In the event of a purely frontal collision, passenger will continue to progress forward until chest impacts steering column or air bag in the event of deployment. In this situation, resultant loading will be focused in the anterior direction of the rib cage. In the event that collision deviates in any way from a solely frontal collision, primary loading on the occupant's thorax will be shifted based on the geometry. An example of such an impact would be a side impact collision. In this geometry, resultant loading will be focused on lateral and anterior of lateral section of the thorax[10]. Injuries associated with loading on rib cage can range from fractured ribs, to pneumothorax, to rupturing of vessels associated with cardiovascular system[2,3,5,6,8,9].

The primary focus of this project will be thoracic impacts in the lateral and oblique direction of impact, Figure 1, which are typical results of side impact collisions. It may be incorrectly assumed that the majority of side impact collisions result in loading

in the lateral direction of impact. However, it has been previously determined that the most common side impact collisions occurs when car 1 is traveling 15 mph and is struck from the side by a car traveling 30 mph[10]. The kinematics of this type of collisions actually result in thoracic impact loading in the oblique directions, Figure 2. Primary Direction of Force (PDOF) loading the thorax is pictured for this collision.

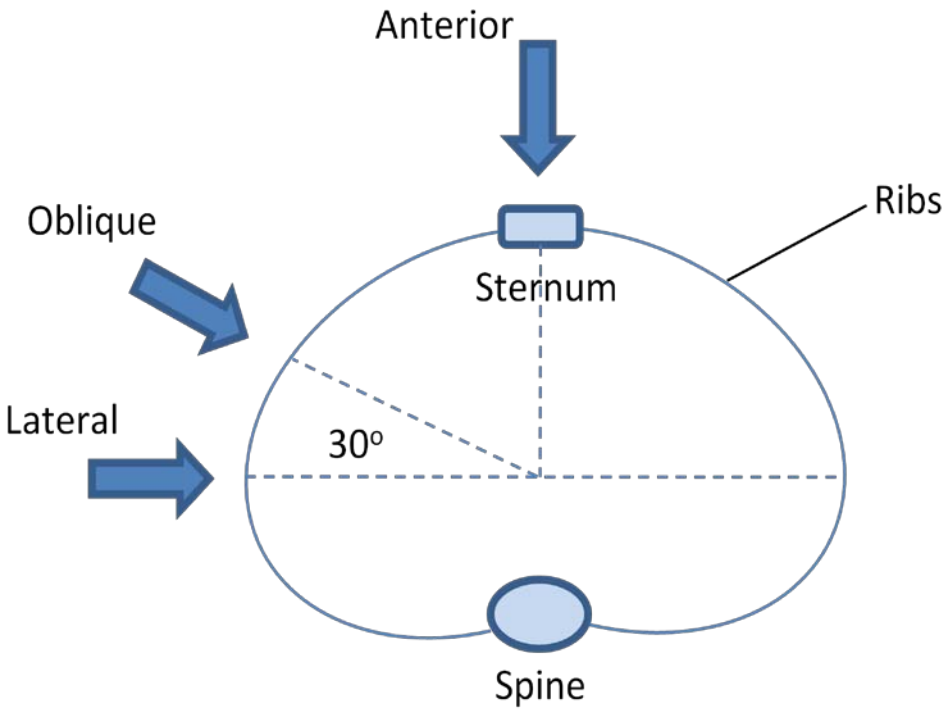

Figure 1. Definition of impact orientations discussed. Impact orientations include anterior, lateral, and oblique.

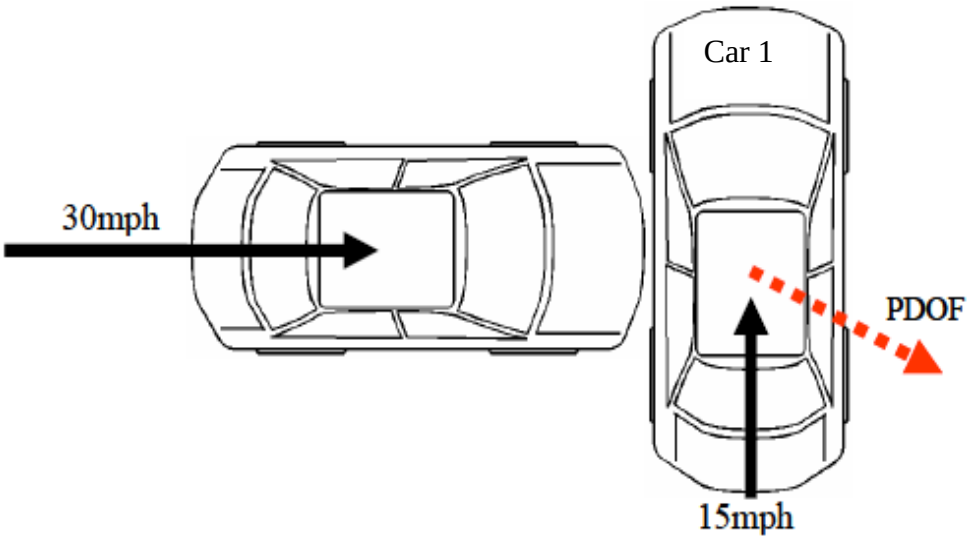

Figure 2. Example of collision that would results in loading on thorax in the oblique directions. Shaw et al (2006).

Current crash test dummy thoracic systems were reviewed in order to gain understanding of the mechanics of crash test dummy thoraxes. Two crash test dummies in particular were researched: THOR NT 50th percentile male frontal impact dummy and World SID 50th percentile male side impact dummy, Figure 3. Immediate similarities between the two dummies were observed. Both dummies were supported by a spine section that was the source of the majority of the mass for the thoracic section. The remainder of the mass was placed in the rib sections. The material for both sets of ribs was a flexible metal that acted to mimic the spring characteristics of the ribs. Dampening material as placed on the ribs of both dummies to mimic the dampening affects of the internal sections of the thorax. These ribs were then covered with a synthetic skin material that was constructed from rubber to mimic the stiffness of the skin. It was

decided that any model of the thorax would have to be constructed by a spring/damper system that is similar to geometry observed in the thorax.

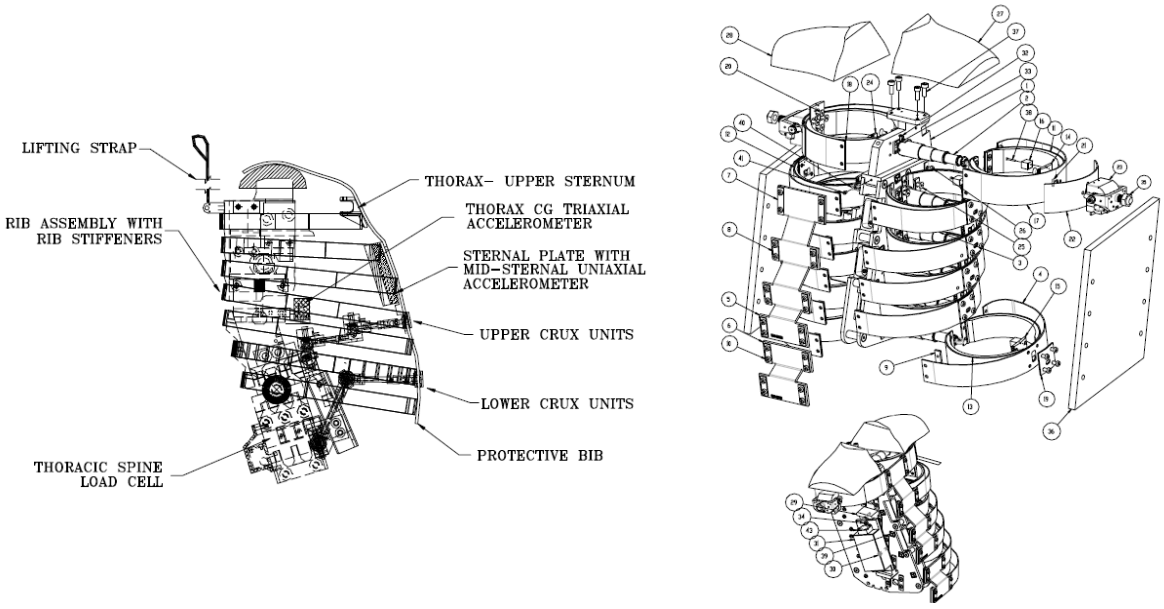

Figure 3. Drawings of THOR NT (left) and World SID (right) crash test dummy thoraxes

A brief review of thoracic anatomy was conducted prior to development of thoracic model. Primary interest was placed on the cross section of the thorax at the level of the 4th thoracic vertebra. At this level the ribs provide the primary structure of the thorax and protect the lungs and heart from damage. The ribs are connected by intercostals muscles. The intercostals along with the diaphragm provide a pressure seal around the lungs that allow for breathing. Surrounding the ribs is the superficial tissue (skin, muscle, fat). In terms of the spring damper system, it is believed based on first impression that the stiffness of the thorax will be controlled by the stiffness of the ribs since they are the firmest structure of the thorax. Alternatively, the dampening of the

thorax will be controlled by the internal organs contained within the ribs based on the presence of blood entering and leaving the thorax during impact. The superficial tissue will contain both spring and dampening affects, however dampening affects of the skin are going to be ignored unless they are determined to be needed based on observation of material used to simulate skin of crash test dummies. It is expected that the thorax will have viscoelastic properties that will affect the stiffness of the thorax based on loading rate as many biological materials do.

1.2 Literature Review

Research has been conducted in an attempt to predict injury and potential risk of fatality to occupants. Initial research was performed by Kroell et al.5, Post Mortem Human Surrogates (PMHS) were placed in a seated position and struck in anterior direction with a pneumatic ram. Varying speeds (14-32 mph) and striker weights (3.6-52 lb) were used in order to characterize the response of the thoracic cavity under multiple loading conditions. The study focused on how the thoracic response of PMHS depended on input variables (speed and striker weight) as well as how responses depended on anthropometric data of each specimen. The data obtained from experimentation was successfully used to calculate stiffness (force vs. deflection) curves for each specimen to provide a baseline for thoracic responses. Additional studies were performed later by Kroell seeking to obtain additional data points in order to better understand the highly varying response of the human thorax[5,6].

Based on data collected by Kroell, Neathery was successful in developing the first mechanical model to attempt to replicate the responses of the thoracic cavity to impacts in the anterior direction. Neathery's mechanical model was based off a previously developed mathematical model by Lobdell including spring/damper systems to model the dominating factors affecting chest deflection such as bending of ribs and tissue compression[7]. Experimental data showed strong correlations between experimental responses to impact and biofedelic corridors developed by Kroell even effectively modeling different responses to varying striker masses and speeds[7]. No model was developed for thoracic response to loading directions that deviated from anterior.

ISO/TR9790 is an international safety standard to determine the biofedelity of crash tests dummies due to impacts in the lateral direction. The only two studies cited in this standard were performed by Eppinger and Viano. Both studies use similar methods to Kroell to measure thoracic response with focus shifted to response from impacts in lateral (Eppinger) and oblique (Viano) directions. Viano concluded that lateral and oblique impacts exhibited similar mechanical responses[9]. Data obtained from experimentation was used to develop international biofedelity corridors for thoracic response to lateral impacts.

Recently, The Injury Biomechanics Research Laboratory (IBRL) at The Ohio State University has begun to reevaluate the assumption that thoracic response in oblique and lateral directions is equivalent. PMHS were impacted in the lateral direction on one side of the thorax and the oblique side on the other in order to allow comparison in

response between the same specimens. In order to not cause destructive damage to the thorax so that thorax could be tested twice, impacts were conducted with a 23 kg pneumatic ram traveling at 2.5 m/s[10]. Impacts of this nature were determined to be below the injury threshold for the average human thorax. Chest band with strain gauges was placed around PMHS in order to measure deflection response of the thorax. Load cell placed on impacting ram recorded the force of impact.

Comparison of lateral and oblique load and deflection showed significant differences between the thoracic responses for the two loading geometries. Average maximum impact force for lateral impacts was 1411 N (plus/minus 181 N) and 1145 N (plus/minus 226 N) for oblique impacts. Average maximum chest deflection measured by chest band also varied with measurements of 36.2 mm (plus/minus 11.4 mm) for lateral impacts and 51.4 mm (plus/minus 7.3 mm) for oblique impacts[10]. Force response vs. time of the thorax impact measured during experimentation was compared to lateral impact biofidelity corridors outlined in the internal standard ISO/TR9790. Biofidelity corridors were scaled to the standard to predict the response of the thorax based on the impact velocity and mass used. It was determined that while lateral impact force response fit well within the biofidelity corridors, oblique force responses did not match the established corridors[10], Figure 4.

1.3 Motivation

Proper understanding of thoracic deflection as the result of impact has application in traffic safety standards. Current crash test dummies are unable replicate the thoracic

response to the wide variety of impact orientations that are observed in actual traffic collisions. Because of the crash test dummies inabilities, primary focus has been placed on replicating thoracic response to impact of common traffic collisions, lateral and oblique for side impacts. It is the hope that completion of this research project will benefit crash safety research in two major ways. First, it will provide an understanding of what mechanically causes the different impact orientations to deviate from each other. Secondly, it will model the thorax as a spring damper model in separate lateral and oblique impact orientations. Such analysis would be the first step towards the design and construction of a crash test dummy that could accurately predict thoracic deflection in the lateral and oblique directions. Meeting both of these goals would go a long way towards providing crash safety researchers with the tools they need to accurately assess the safety of modern cars in their effort to reduce traffic fatalities and severe injury.

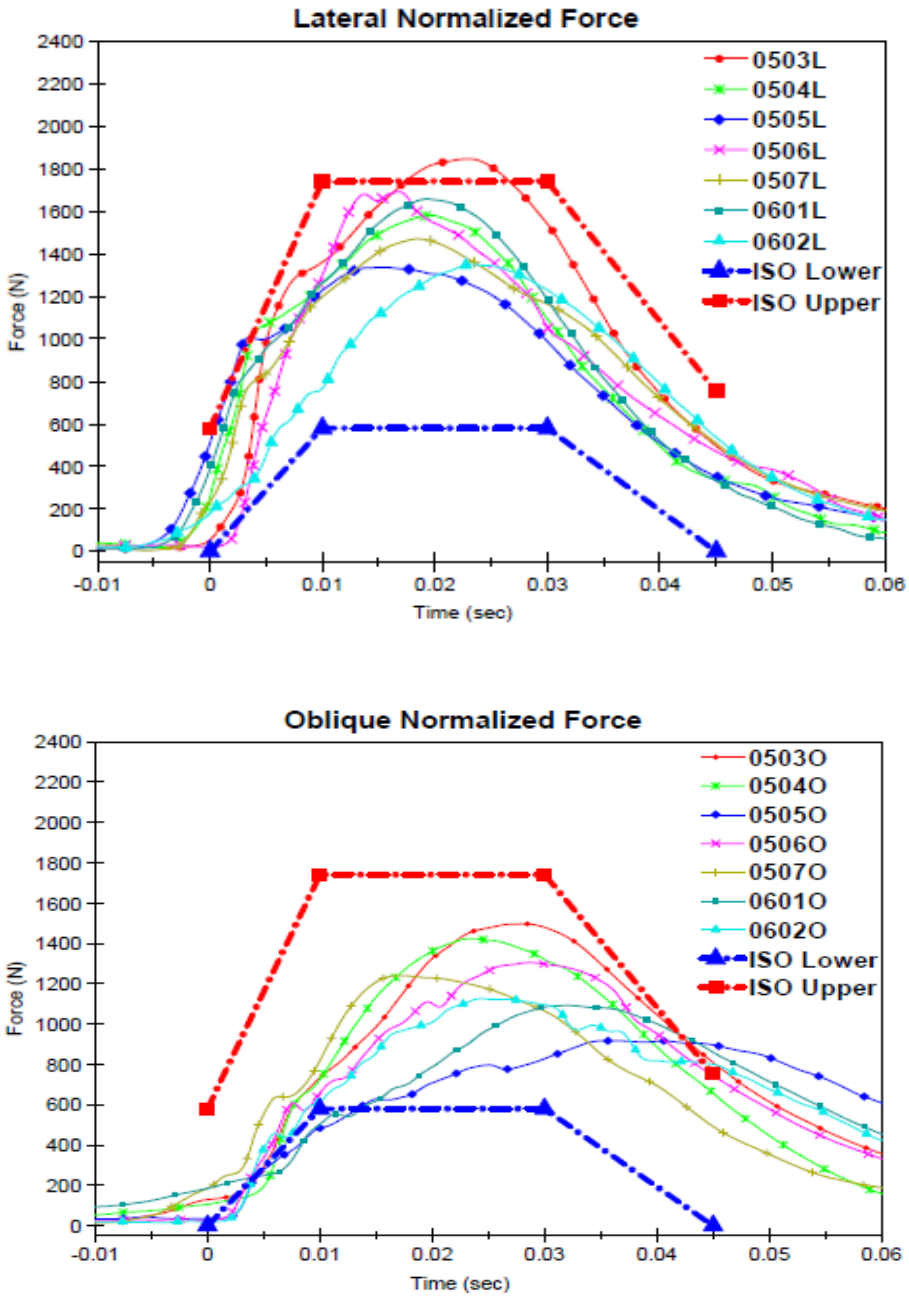

Figure 4. Comparison of force response with respect totTime for PMHS when impacted in the lateral (top) and oblique (bottom) orientations. ISO corridors are based off ISO/TR9790 standards for side impact collisions scaled to the specific parameters in the low speed testing performed by Shaw et al (2006).

1.4 Project Objective

The objective of this project is to develop a mathematical model to simulate and predict thoracic response to impact in both the lateral and oblique directions. Mathematical model will be developed similarly to the model produced by Lobdell in order to model thoracic response in anterior impact direction. The model will be created using a spring/damper system that will simulate the response of the thorax through a Matlab SimMechanics program. Matlab model will be able to run simulation of thoracic response based on inputs such as the ram position data as well as parameters defining the constants of spring and dampers of the model. The SimMechanics model will then be optimized to experimental data obtained in the IBRL at The Ohio State University for side thoracic impacts in the lateral and oblique directions. The response generated by the Matlab SimMechanics simulation will then be compared to data collected in the IBRL in order to determine effectiveness of model. It is the hope that modeling the thorax during impact will provide an understanding of what mechanically is changing when the thorax is impacted in the lateral as opposed to oblique directions and generation of a spring damper model that could be used to simulate thoracic deflection in the lateral and oblique impact orientations.

CHAPTER 2

PREVIOUS THORACIC IMPACT EXPERIMENTS

This section outlines the previous thoracic impact testing procedures and results completed in the IBRL. Data from these experiments will be used as the sole source of data used in thoracic simulation. Completion of thoracic impact experiments was performed by Josh Shaw (Low Speed Impacts) and Matt Long (High Speed Impacts) under the direction of Dr. John H Bolte IV.

2.1 Experimental Set Up and Procedures

The source of data for this model is based on experimental work previously completed in the IBRL (Injury Biomechanics Research Lab) at The Ohio State University under the direction of John Bolte IV. Experiments included the use of PMHS (Post Mortem Human Surrogates). PMHS were obtained through the willed body donation program at The Ohio State University and all testing protocols were approved by Ohio State's Internal Review Board. . PMHS were placed in a seated position by suspending the PMHS from the top of the assembly using a specially designed harness that is attached around the head of the surrogate. The arms were rotated 90 degrees from anatomical position in the anterior direction, exposing the lateral sections of the thorax, Figure 5. Controlled impact force was generated using a pneumatic ram. The impacting

portion of the ram was able to be removed and replaced based on needs of the test step up. Two ram faces were used in the experimental set ups described for this testing: a rounded face and a square face. The rounded face was constructed with a .5 in fillet around the border of the ram in order to reduce the likelihood that the ram would produce rib fractures since non injurious impacts were desired for the low speed experiments. Ram was positioned at the level of the 4th thoracic vertebra. Speed of ram is able to be controlled based on air pressure used for actuation applied prior to impact with the PMHS. Orientation of impact was either lateral or oblique, Figure 6.

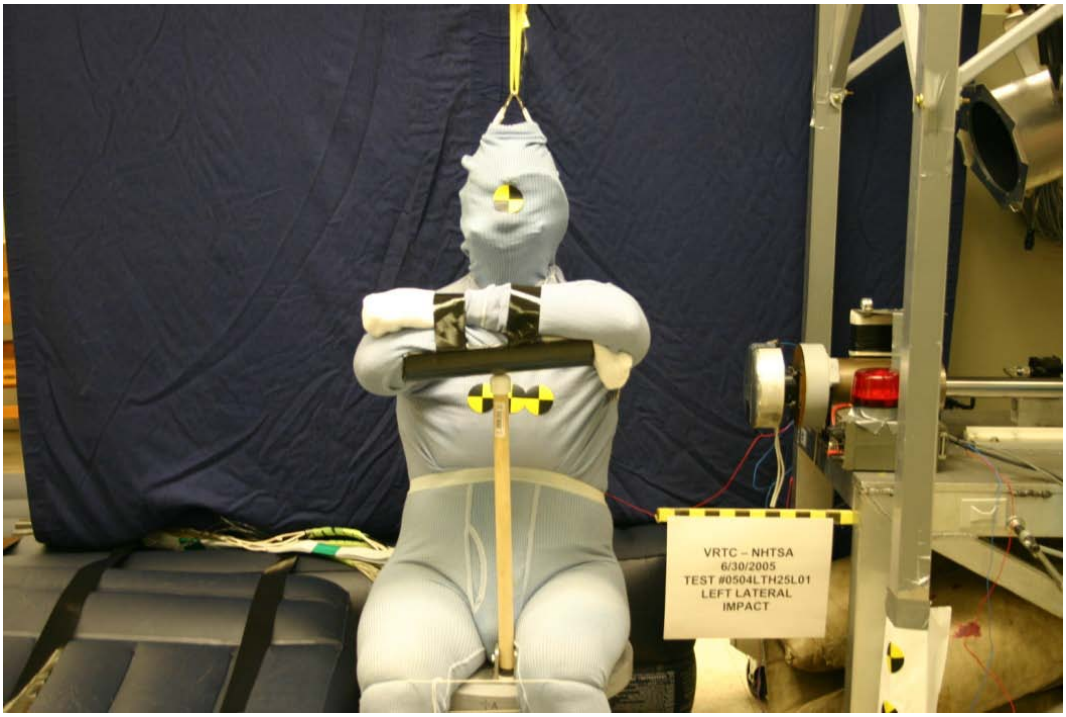

Figure 5. Picture of PMHS in test set up prior to actuation.

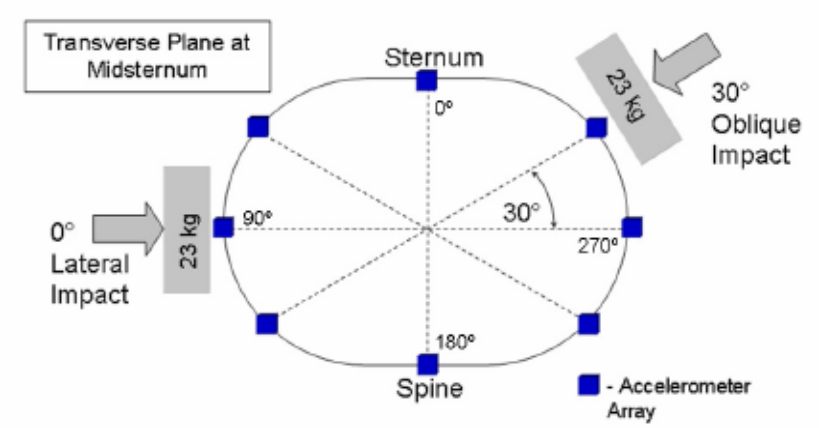

Figure 6. Definition of lateral and oblique impact and position of accelerometer arrays. Shaw et al. 2006

Each experiment was started by pressurizing the pneumatic impactor to desired levels. When pneumatic ram was actuated, electrical sensors were in place on the ram and the PMHS. When the ram made first contact with the PMHS, contact between the sensors on the PMHS and ram completed a circuit. This moment was defined as time zero. Prior to time zero, the head harness supporting the weight of the PHMS was released as ram contacts additional switch. This allowed the PMHS to respond similarly to a seated person. PMHS was then impacted and ram continued forward until maximum extension was reached. At this point, PMHS was free to continue free fall until the surrogate was caught by Secondary Impact Prevention Unit (SIPU), concluding the test. This testing procedure was completed under two different loading conditions: high speed and low speed. The low speed test (2.50 m/s) was completed below injury threshold so that the surrogate could be impacted on both sides of the thorax. As such, rounded face of impactor was used in order to reduce the likely hood of rib fractures and preserve the thorax for a second impact. This allowed for direct comparison between lateral and

oblique impacts. Side of impact (right or left) was alternated for each PMHS impacted under low speeds. Low speed impacts were performed on 7 surrogates for a total of 14 experiments (7 lateral and 7 oblique). After comparative study was completed, high speed tests (4.50 m/s) were completed to quantify chest deflection for injurious impacts on 6 surrogates for a total of 6 experiments (3 lateral and 3 oblique). Increased speed of impacting ram was used in order to generate appropriate impacting forces to observed injurious rib fractures.

2.2 Experimental Measurements

PMHS were instrumented in order to take several key measurements for characterizing the impact. All measurement techniques followed the same coordinate systems outlined by SAE J211 standards for biomechanics data collection for use in crash test safety. Coordinate system required x to point in anterior direction, y to point to the right, and z pointing in the inferior direction, Figure 7. The pneumatic ram was equipped with sensors to measure force in the x, y and z directions, moments about the x, y and z axes, as well as acceleration in the y direction. Motion of the ram was constrained to the y direction, so measurements of the x and z acceleration directions would not have been useful. In addition the instrumentation included a potentiometer rigidly fixed to ram base in order to measure the position of the ram as it was actuated through time.

Each surrogate was instrumented with accelerometers in multiple locations. On the spine, accelerometer arrays were placed on the spinous process of the 2^{nd}, 4^{th}, and 12^{th} thoracic vertebra. Similar accelerometers were placed on the sternum at the level of the

4th thoracic vertebra. In addition, 6 accelerometer arrays were placed on the ribs of each surrogate at the level of the 4th thoracic vertebra. Locations of the six accelerometers were right and left lateral, right and left anterior oblique and right and left posterior oblique, Figure 6. Accelerometer arrays contained 3 accelerometers measuring acceleration in the x, y, and z direction. Each location of insertion of accelerometer arrays was sutured closed after attachment to ribs in order to minimize affecting the structural integrity of soft tissue. Accelerometer arrays were only instrumented on surrogates that underwent low speed impacts. For high speed tests only, strain gauges were placed directly on multiple ribs in an attempt to estimate the exact time of rib fracture during the experiment. Strain gauge placement varied for each experiment, but typically were placed on ribs at the level of T2-T10. In order to measure chest deflection at all points around surrogate, a chestband developed by Denton ATD was placed around the surrogate at the level of the 4th thoracic vertebra. Chestband consisted of 40 strain gauges placed at 1 inch intervals. Strain gauge measurements of curvature around the subject would later allow for development of x y profiles of the chest through the entire test.

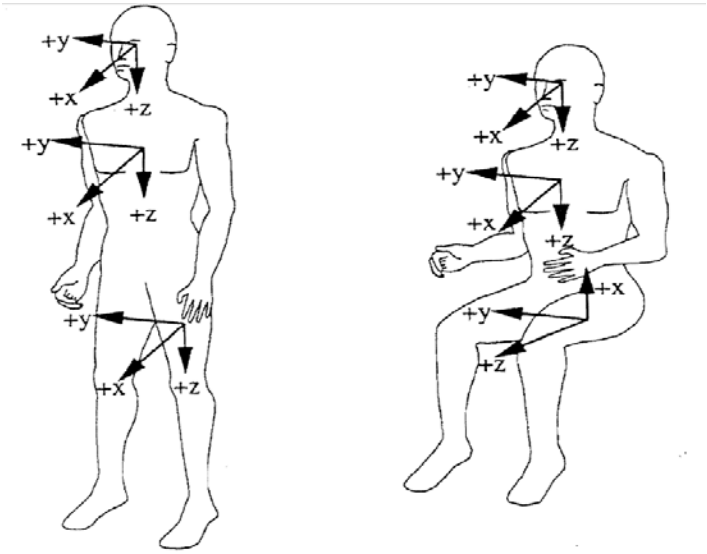

Figure 7. Definition of surrogate coordinate system for each test. Coordinate systems is based on SAE J211 for biomechanical research.

2.3 Thoracic Impact Experimental Results

The following outlines the experimental results as reported by the IBRL at The Ohio State University of thoracic impact in the lateral and oblique impact directions to low speed (2.5 m/s) and high speed (4.5 m/s) impacts.

2.3.1 Low Speed (2.5 m/s) Impacts

Contrary to initial findings during previous thoracic impact testing, a significant difference was observed between impacts in the lateral and oblique directions for low speed impact testing. Results showed that oblique impacts experience statistically significant higher deflection for similar impact speeds, Figure 8. Deflection is defined as the difference between current thoracic depth and initial thoracic depth. Since injury to

the thorax during an automobile collision is estimated based on thoracic deflections of crash test dummies and current crash test dummies are designed to deflect similarly in lateral and oblique impact directions, these results implied that current crash test dummies might be underestimating thoracic deflection for oblique impacts and as a results, underestimating injury.

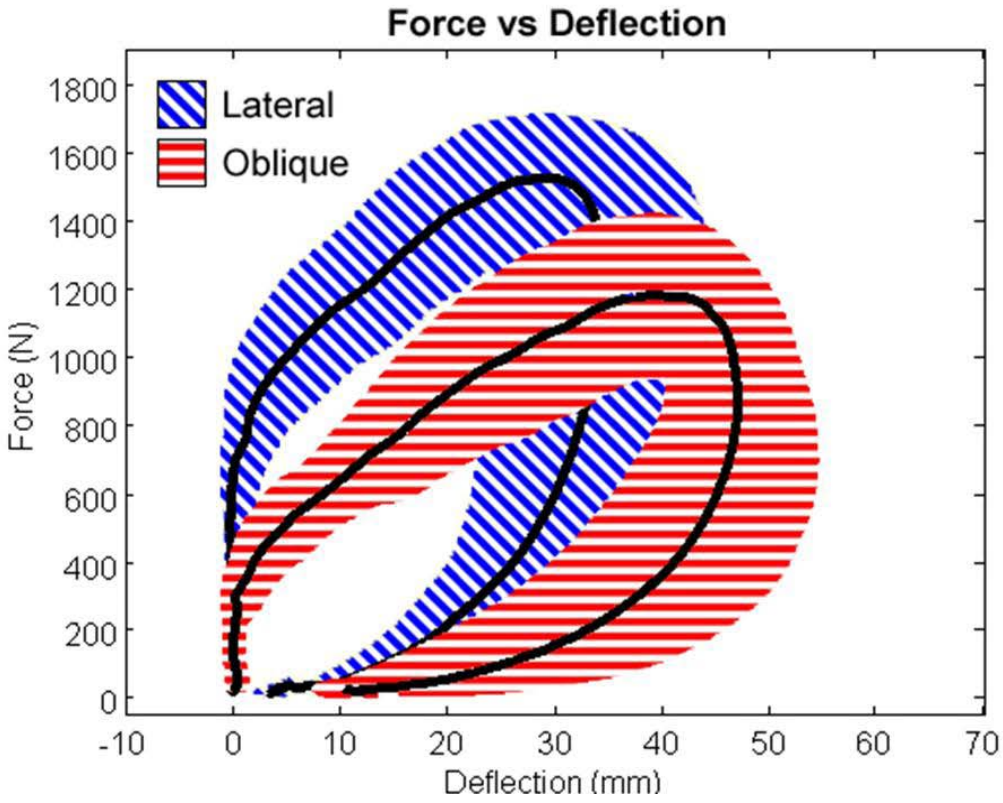

Figure 8. Average experimental stiffness (force vs. deflection) curves for low speed impacts in lateral and oblique directions. Shaded area around curves represents one standard deviation away from average. Shaw et al. (2006).

2.3.1 High Speed (4.5 m/s) Impacts

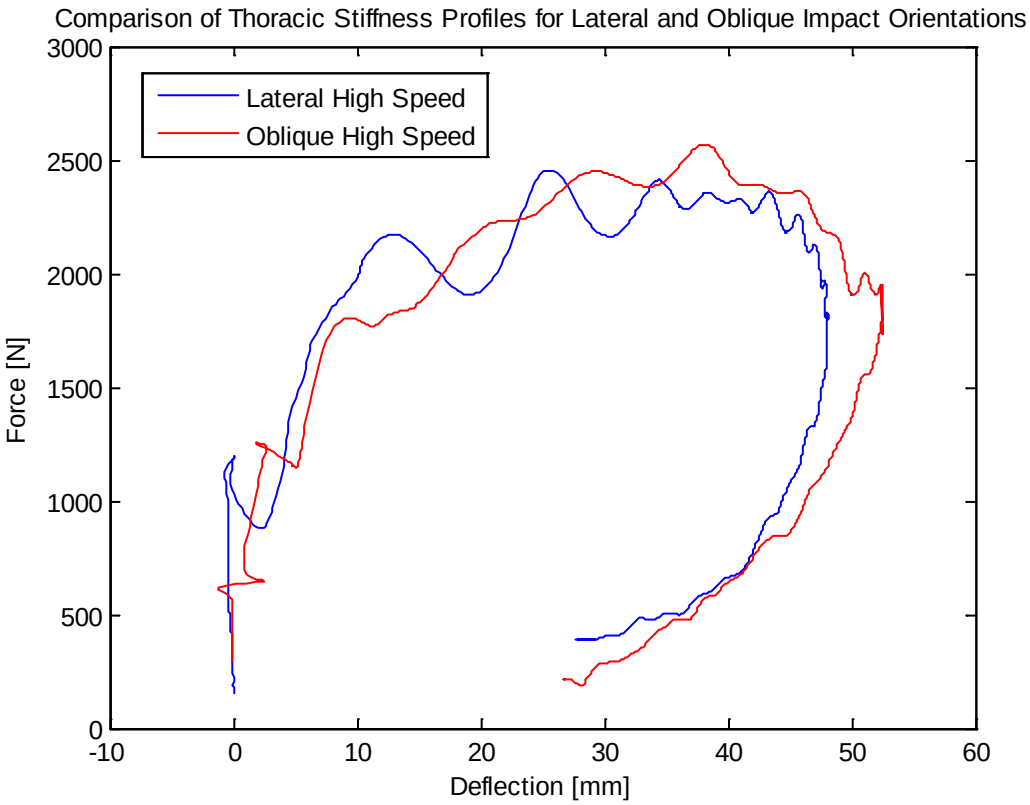

Figure 9. Average Experimental Stiffness (Force vs. Deflection) Curves for High Speed Impacts in Lateral and Oblique Directions

Comparison of average experimental thoracic stiffness curves in lateral and oblique directions, Figure 9, for high speed (4.5 m/s) impacts does not show the same significant difference between lateral and oblique impact directions. Quite the opposite is observed. Both impact force and thoracic deflection between the two impact directs are of similar magnitude. Almost identical procedures were used when collecting both high speed and low speed thoracic impact experimental data. The only difference between the

two experimental set ups is the impactor face used and the instrumentation placed on the PMHS. As mentioned previously, high speed experiments used square impactor as opposed to rounded face impactor for low speed impacts. For low speed impacts, 6 accelerometer arrays were placed directly to the ribs at the level of impact. Alternatively, for the high speed impacts strain gauges were placed on ribs 3 through 10 on side of impact. Additionally, the vasculature of the thorax when re-pressurized in order to simulate conditions that could result in traumatic rupture of the aorta. Re-pressurization was completed by inserting catheters into the primary artery and veins of the heart and filling these vessels with pressurized saline. It is not believed that these changes to the experimental set up could account for the different results from the two set ups. Based on results from high speed impacts, it is understood that the response of the human thorax to impact is extremely rate dependent and more complicated that initially understood.

2.4 Summary

Experimental data for the thoracic response to impact in the lateral and oblique impact orientations was completed at two impacting speeds: low speed (2.5 m/s) and high speed (4.5 m/s). The results of these tests are contradictory. The results of the low speed impacts shows that the human thorax exhibits differing responses in the lateral and oblique orientations. These results are not observed in the high speed data. Additional research into lateral and oblique impacts needs to be completed in order to develop a better understanding of the response of the human thorax for crash safety research.

CHAPTER 3

ADAMS MODELING OF ACCELEROMETER ARRAYS

Modeling of accelerometer arrays was completed with hopes of understanding how the skeletal structure of the thorax responds to impact in the lateral and oblique directions. As stated previously, accelerometer arrays were placed at specific locations directly on the ribs of each PHMS impacted under the low speed impact criteria. The data from these accelerometer arrays was used to simulate the motion of the rib cage without inclusion of soft tissue deformation due to low speed impacts.

3.1 ADAMS View Modeling Methods

Adams View is a motion simulation program primarily used for mechanical systems. However, this program also allows users to create models based on experimental data. Because of its capabilities in this area, Adams view was used to model the accelerometer arrays placed on the surrogates. Since all crash test dummies consist primarily of rib elements to simulate chest deflection and an outer coating of synthetic skin, an accurate understanding of how the rib cage deforms is of great use for developing an accurate model. It was decided that modeling the accelerometers placed on each surrogate's ribs would be the best way to determine deflection of the rib cage excluding deflection of the superficial tissue.

As mentioned previously, 6 accelerometer arrays were placed around the rib cage and 1 on the sternum. All of these accelerometer arrays were placed at the level of the 4^{th} thoracic vertebra. In addition three accelerometer arrays were placed on the 2^{nd}, 4^{th}, and 12^{th} thoracic vertebrae. All of these accelerometer arrays measured acceleration in the x, y, and z directions. In order to model accelerometers, blocks the approximate size of the accelerometer blocks were created in Adams, the initial position of these blocks was based on anthropometric data that was specific to each surrogate and recorded at the time of testing. The result is a base model that consisted of vertical line of 3 accelerometers representing the spine and a hoop of 8 accelerometers representing the sternum and specific points on each rib, Figure 10.

Since each surrogate initially started from rest, accelerometer data needed to be zeroed. A Matlab program was created that imported accelerometer data, zeroed the accelerometer data, filtered the data based on SAE J211 standards for biomechanical research, and converted to appropriate format to be imported into Adams. Accelerometer data was zeroed by averaging accelerometers reading up until point of impact and subtracting the average from the accelerometer data. Processed data was then imported into Adams View.

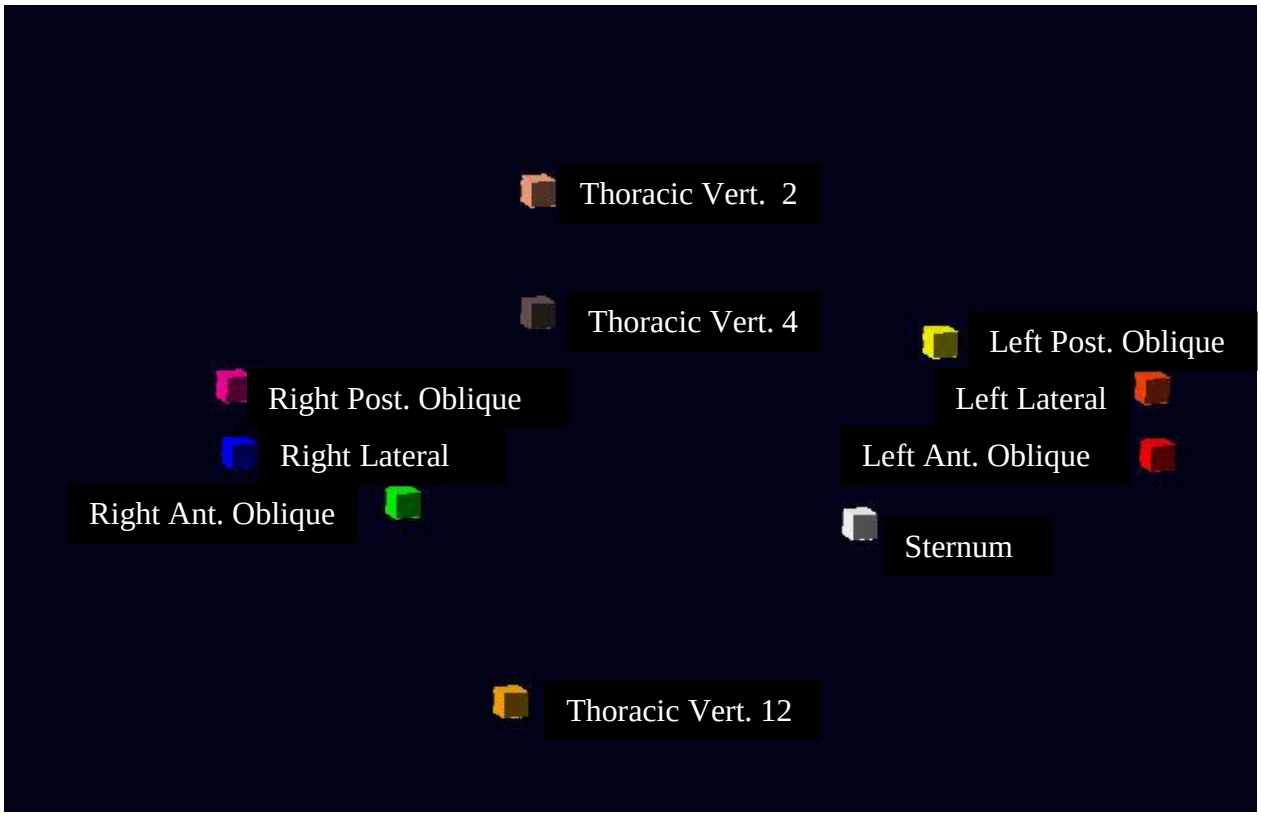

Figure 10. Picture of ADAMS view model of accelerometer arrays in initial position. Each array is labeled based on its position on the PMHS.

In ADAMS view splines of each set of data was created. Accelerometer data was then numerically integrated twice to obtain the position functions for each accelerometer in the x, y, and z directions. Initial conditions of position and velocity were assumed to be zero since PHMS were motionless until impacted by ram. Next, each block in Adams View was constrained to move as outlined by experimental data. Measurements of deflection were taken between each block based on the orientation of impact (Lateral or Oblique) as outlined in Figure 11.

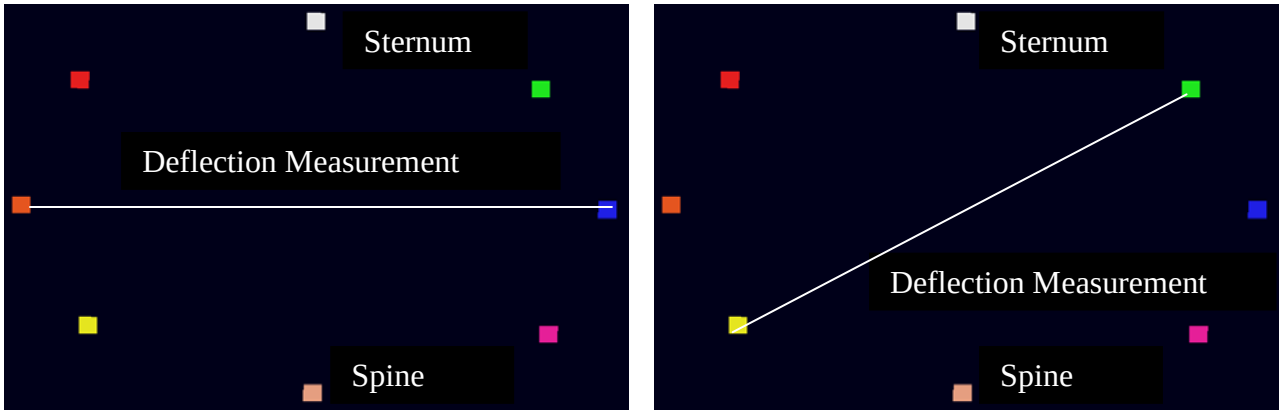

Figure 11. Definition of chest deflection measurements taken from ADAMS view model in lateral (left) and oblique (right) directions

3.2 ADAMS View Modeling Results

ADAMS post processing allowed for analysis of deflection measurements between appropriate accelerometer blocks. Example measurements of deflection for a single test can be observed in Figure 12. Graphs and data from all ADAMS view work may be found in appendix A.

Verification of ADAMS modeling technique can be observed through observation from the simulated data. For example, ADAMS modeling deflection measurements show that maximum compression of the thorax in lateral and oblique directions corresponds strongly to time of maximum compression observed from the chestband deflection measurements. Also, general appearance of motion of accelerometer arrays through time is consistent with the general understanding of how a thorax deflects during impact, Figure 13.

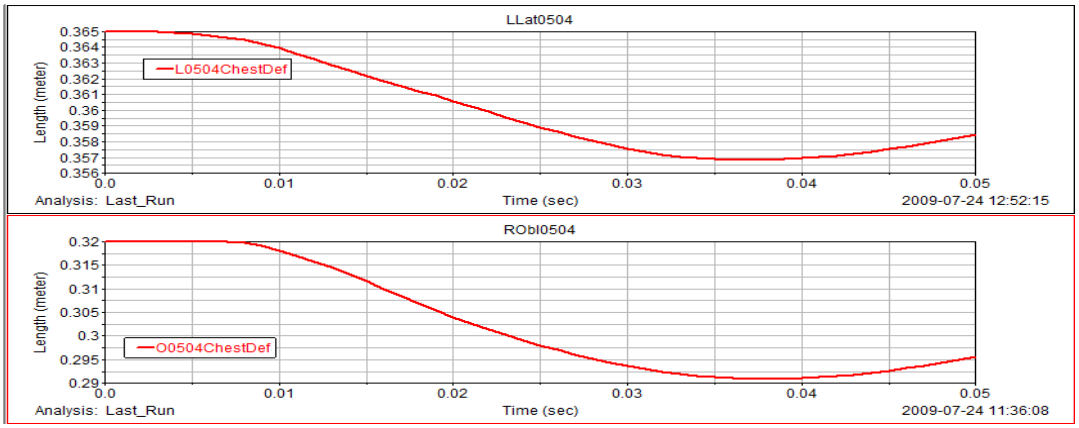

Figure 12. Resultant chest deflection measurements for test 0504 in lateral (top) and oblique (bottom) directions based on ADAMS View modeling of accelerometer arrays

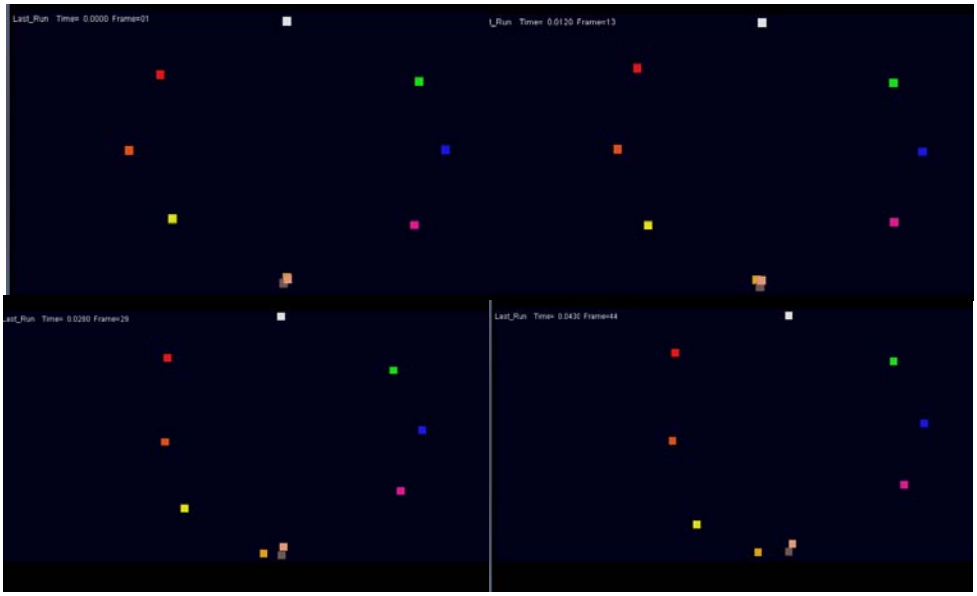

Figure 13. Progression of accelerometer array positions through time as modeled by ADAMS View for sample low speed thoracic impact Lat 0503. Lat 0503 was a lateral orientation impact to the left thorax

As can be seen in figure 13, which is a left lateral impact, motion of accelerometer arrays modeled in ADAMS view maintain a very similar shape throughout the entire time of impact with the exception of the left side of the thorax which

compresses inward as a result of impact from the ram. Figure 10 reveals a label of each accelerometer array's placement on the PMHS. Identical color schemes are used for all ADAMS view modeling to denote the position of each accelerometer array.

3.3 Comparison with Chestband Deflection Measurements

Despite observed correspondence of ADAMS view modeling with expected results, the only way to prove or disprove the accuracy of ADAMS view modeling is to compare the results with measurements taken from a known accurate method of determining thoracic deflection. For the thoracic impact tests performed in the IBRL, chestband measurements were the primary source of thoracic deflection measurements. Direct comparison between measurements from ADAMS view modeling and chestband measurements is not completely possible since chestband measurements include deflection of the soft tissue superficial to the rib cage of each surrogate while ADAMS view modeling does not. However, comparison of results from these two system of measures will either provide more support for ADAMS view method of determine skeletal deflection as a result of impact or disprove its accuracy.

3.3.1Chestband Modeling

As previously mentioned, a primary source of thoracic deflection measurements was the thoracic chestband developed by Denton ATD. Each thoracic chestband consists of 40 strain gauges placed at 1 in intervals and is wrapped around the thorax at desired level, for these experiments it was at the level of impact. Through strain gauge

measurements it is possible to measure the curvature of the thorax throughout the entire time interval of impact. The use of Crashstar Matlab program developed by NHTSA converts these measurements of curvature into vector positional data outlining the position of each strain gauge placement relative to the position of the spine, Figure 14.

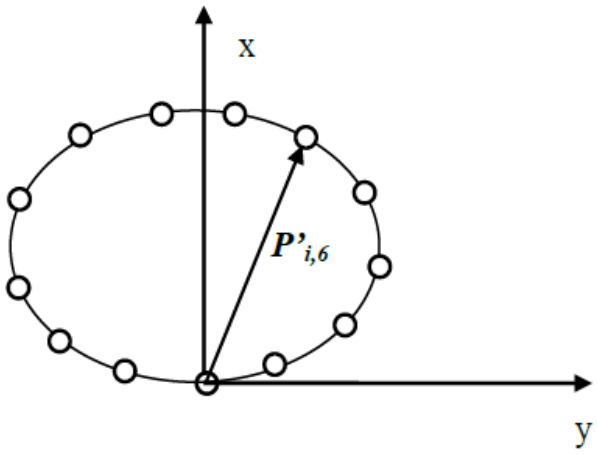

Figure 14. Example of vector data reported for chestband after Crashstar processing. Processed data consisted of vector quantities that measured the distance from the spine gauge to each gauge within the chestband. Circles along encompassing chestband hoop in figure represent strain gauge positions.

Based on the output from Crashstar, a Matlab program was created that calculated the resultant vectors between each of the strain gauges. Matlab then found the maximum thoracic deflection observed during impact between any of the strain gauges. Unsurprisingly, maximum deflection was always observed to follow the line of impact through the surrogate as noted in records from day of test. The Matlab program then displayed the graphs of shape of the thorax before impact and at the point of maximum

deflection. Figure 15 reveals examples of thoracic deflection for both impact geometries: lateral and oblique. Once location of maximum deflection was determined, the resultant vector between the two gauges where maximum deflection occurred was calculated at each time interval throughout the duration of the test. Resultant distance was calculated and subtracted from the initial distance between the vectors in order to develop a deflection profile with respect to time. These methods were repeated for all of the low speed impact tests.

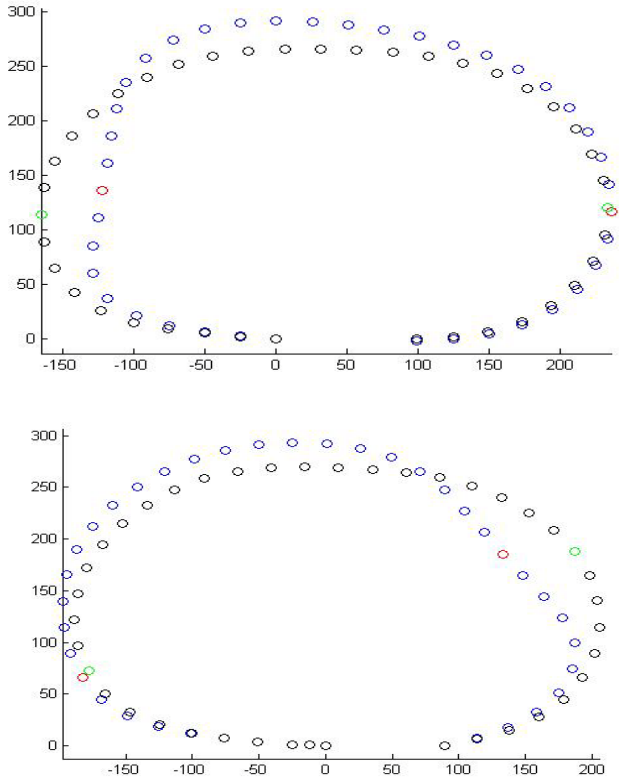

Figure 15. Chestband profiles (x and y) for test 0504 at initial position and point of maximum deflection as measured by the chestband. Chestband measures chest deflection of a cross section of the chest in the x and y plane at the level of the 4th thoracic vertebra. Green gauge markers show the line of impact at its initial position and red markers show the line of impact at its most compressed point. Units in millimeters.

3.3.2 ADAMS view and Chestband Comparison with Interpretation

For the purposes of this report, thoracic deflection is defined as the difference between the initial depth of the thorax along the line of impact and the depth of the thorax along the line of impact at a specific time interval during impact of the thorax, while thoracic compression is defined as the percentage of the maximum deflection of the thorax along the line of impact relative to its initial depth.

$$deflection = chest\big|_{t=o} - chest\big|_{t} \qquad (1)$$

$$compression = \frac{chest\big|_{t}}{\left(chest\right)_{\max}} \qquad (2)$$

Total thoracic deflection is measured by the chestband measurement system and includes soft tissue compression while skeletal thoracic deflection is measured by ADAMS view simulation and represents the compression of the rib cage without soft tissue compression. Soft tissue compression is the difference between total thoracic deflection and skeletal thoracic deflection. Tables 1 and 2 represent a comparison between the total and skeletal deflection and compression measurements in order to determine the validity of ADAMS view modeling technique.

Table 1. Total deflection, skeletal deflection, and soft tissue deflection for all 14 lateral and oblique low speed thoracic impacts. Skeletal deflection and soft tissue deflection for oblique impact 0503 is not reported because data was not complete to generate model in ADAMS View.

	Total Deflection [mm]			Skeletal Deflection [mm]			Soft Tissue Deflection [mm]	
	Lateral	Oblique		Lateral	Oblique		Lateral	Oblique
503	31.5	56.4		NA	46.4		NA	10.0
504	40.0	44.9		8.2	29.1		31.8	15.8
505	34.1	64.7		14.8	54.4		19.3	10.3
506	30.5	51.9		10.2	47.5		20.3	4.4
507	44.7	52.3		22.9	37.2		21.8	15.1
601	34.4	49.1		15.0	23.7		19.4	25.4
602	68.3	44.9		15.6	31.7		52.7	13.2
Avg:	40.5	52.0		14.5	38.6		28.1	13.5

Table 2. Total thoracic compression and skeletal thoracic compression for all 14 lateral and oblique low speed thoracic impacts. Skeletal compression for oblique impact 0503 is not reported because data was not complete to generate model in ADAMS View.

	Lateral			Oblique	
	Skel Comp	Total Comp		Skel Comp	Total Comp
503	NA	9.13%		15.62%	17.26%
504	2.25%	10.01%		9.09%	11.75%
505	3.40%	10.04%		5.00%	19.94%
506	3.11%	8.77%		15.94%	15.04%
507	7.36%	13.04%		12.36%	15.92%
601	4.13%	10.44%		6.85%	15.08%
602	4.47%	18.47%		9.49%	13.27%
Avg	4.12%	11.42%		10.62%	15.47%

Observations from tables 1 and 2 show that not only is the total thoracic deflection greater for oblique impacts, but also the skeletal deflection (deflection of the rib cage). Alternatively, the majority of lateral orientation impacts is absorbed in soft tissue deflection. This is an expected result based on the anatomy of the thorax. As can be seen from figure 16, there is significantly more soft tissue (including skin, fat, and muscle) at the point of lateral impacts. It is believed that larger values of soft tissue deflection are at least in part due to more soft tissue concentrated at the lateral impact direction. Errors associated with modeling of skeletal thoracic deflection in ADAMS view will be discussed in the following section.

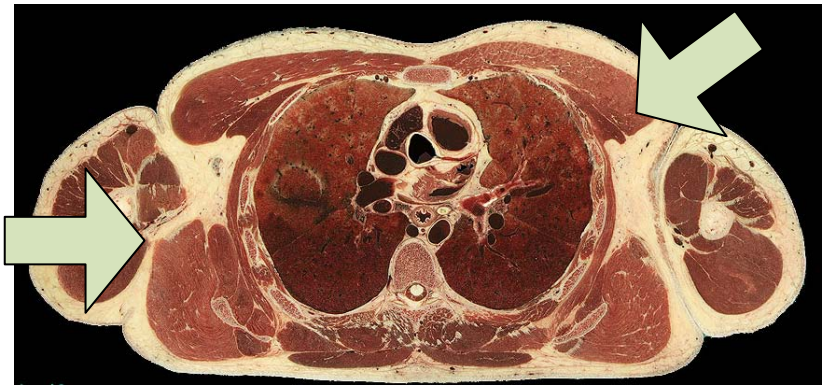

Figure 16. Thoracic cross section of the thorax at the level of impact. Cross section includes arms which should be ignored when comparing lateral and oblique soft tissue composition.

3.4 Conclusions and Shortcomings

Measurements through ADAMS view provided the best possible estimate of skeletal deflection based on impact with the information provided. However,

instrumentation of each surrogate was not complete and did not record enough information to develop the understanding of skeletal deflection that was desired. Firstly, the accelerometers were only placed at eight locations around the surrogates. This means maximum deflection measurements could only be taken at these points regardless of whether or not it was the point of maximum deflection. While it was the goal of instrumentation that the accelerometers be placed as close to the impact sight at possible, in reality there is no guarantee that the accelerometer was actually measuring at the point of maximum deflection. Fortunately, comparison with chestband data showed that approximate point of impact was consistent with desired point of impact that was outlined on reports from the day of testing. These results imply that this source of error was minimized.

The largest source of error while developing this model is the lack of rotational data from each accelerometer array. Once the thorax is impacted, the thorax not only rotates around its center of gravity, but also changes shape because of how the thorax deflects. Both of these movements will cause the accelerometer array's coordinate system to shift relative to the body coordinate system outlined in the introduction. However, without angular measurement sensors, it is impossible to quantify how the coordinate systems shift relative to each other. Which means that the accelerometers will slowly begin to drift from their actual positions as the model runs through modeling the impact. Because of this, the model was only run for 50 milliseconds which was determined to be enough time to observe maximum skeletal deflection, and also minimize accelerometer array drifting. Current research in the IBRL that uses accelerometer arrays have included

angular rate sensors to compensate for this error. However, experimental data that is the source of this model was collected before implementation of these policies. It is believed that lack of angular rate measurements will have a much more profound impact on measurements of skeletal deflection in the oblique direction since the oblique direction has been observed to show more rotation with impact.

These sources of error are impossible to account for or quantity in ADAMS view modeling. Even with attempts to minimize error due to lack of angular sensor measurements, it is understood that measurements from this model are at best only an estimate of skeletal deflection based on impact. However, with no other means of measuring skeletal deflection, the model was taken as the best means of isolating skeletal deflection. It was the initial desire of modeling accelerometer arrays in ADAMS view to produce a secondary point of comparison for simulating thoracic deflection in addition to total thoracic deflection measurements from the chestband sensors. However, the accumulation of errors during performing ADAMS view modeling that could not be accounted for as well as the concern that ADAMS view modeling is underestimating thoracic deflection required that using skeletal deflection as a point of validation of thoracic deflection simulation must acknowledge the limitations of using ADAMS view to model thoracic deflection.

3.5 Summary

ADAMS view modeling of accelerometer arrays was performed with the hopes of quantifying skeletal thoracic deflection of the thorax to low speed impacts in the lateral

and oblique directions. Results were reported and compared to measurements of total thoracic deflection taken from chestband measurements. Comparison showed promise that ADAMS modeling technique was able to somewhat accurately measure skeletal deflection. However, lack of angular rate data and the accumulation of other errors that cannot be counted are acknowledged and using results from ADAMS view modeling will only be used as a secondary point of comparison when validating thoracic deflect simulation. Total thoracic deflection should be the primary point of comparison.

CHAPTER 4

DEVELOPMENT OF THORACIC IMPACT SIMULATION

Development of a SimMechanics model of thoracic deflection response to impact force is outlined. SimMechanics model is based on the previous model of thoracic deflection developed by Lobdell[7]. Updates to the original thoracic deflection model are minimal and outlined. SimMechanics model is run and evaluated based on experimental data from either low speed or high speed thoracic impacts. Processing of experimental data for use in each simulation is outlined.

4.1 Original Simulation Model and Reasoning

Spring damper system that is being used to simulate the deflection of the thorax is based on previous research completed by Lobdell et al. Lobdell et al. simulated thoracic deflections in the anterior direction. Lobdell's model assumed that various structures within the thorax including the skin, ribs, and diaphragm in conjunction with viscoelastic properties would affect the mechanic properties of the thorax. As such, his preliminary model consisted of elements to estimate these interactions, Figure 17. Lobdell's spring/damper model was used as a starting point for modeling thoracic deflection in the lateral and oblique directions.

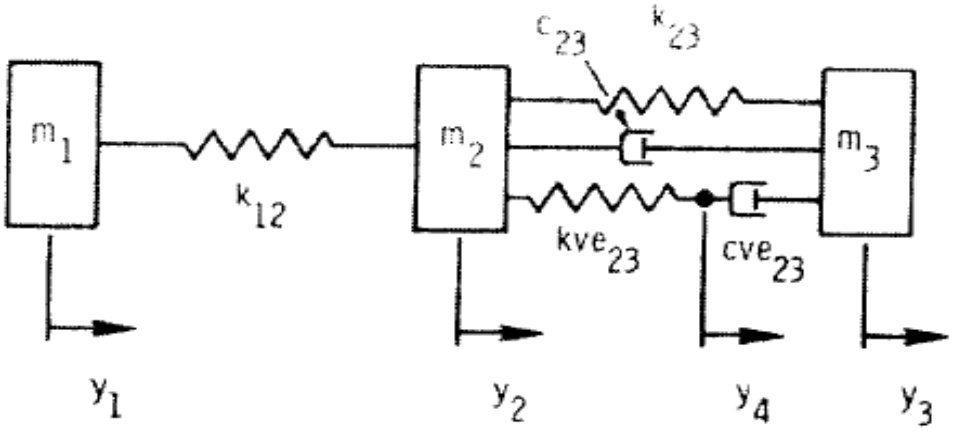

Figure 17. Initial proposed spring/mass/ damper model proposed based on thoracic simulation performed by Lobdell et al[7].

Reasoning associated with each element of the spring damper model are as follows:

- M1—M1 represents the impacting mass acting on the thorax. For the experimental set up developed in the IBRL, the impacting mass is the mass of the pneumatic ram used to strike the thorax and can easily be calculated by weighing the ram. Since high speed and low speed tests use slightly different impacting rams, the weight of m1 will be slightly different for the two conditions after weighing the two rams, the value of m1will be a constants 24.82 or 23.97 kg for low speed and high speed impacts, respectively.

- M2 and M3 –The sum of m2 and m3 represent the effective mass of the thorax during impact. The effective mass is a measure of how the weight of the thorax

influences the motion of the impacting ram. Calculation of the effective mass of the thorax is based on the principle of conservation of momentum. Since momentum is conserved throughout the impact of the thorax, the impacting ram and thorax are assumed to act as a two mass, colliding system. Since acceleration of the impacting ram and mass of the impacting ram are known and acceleration of the thorax can be determined through accelerometer arrays placed on the spinous process of the 4th thoracic vertebra, it is possible to calculate the effective mass of the thorax. The equation for effective mass of the thorax is shown in equation 3.

$$m_{eff} = \frac{m_p\left(\int_0^{T0} a_p dt - \int_0^{T} a_p dt\right)}{\int_0^{T} a_c dt} \qquad (3)$$

In equation 3, m_p and a_p are mass and acceleration of the impacting ram, respectively and a_c is the acceleration of the PMHS thorax. T is time with value of zero signifying the beginning of the test, To as experimental time zero defined by contact of the thorax with the ram, and T as the point in time that the effective mass is being calculated. Effective mass of the thorax varies for each impact experiment. The effective mass of each thorax are grouped into four groups: low speed lateral, low speed oblique, high speed lateral, and high speed oblique. The effective masses of each group are averaged in order to determine the mean effective mass from each group. The mean

effective mass is from each group is defined as the summation of m2 and m3 when performing a simulation from that respective group, Table 3.

As mentioned previously, typical crash test dummy thoraces are developed by constructing a central mass of the thorax that is used as the primary support of the crash test dummy's upper body and contains the majority of the weight of the thoracic section of the dummy. This idea is replicated in the thoracic spring damper model proposed as m3. However, the rib elements of the crash test dummy have a certain amount of inertia properties that need to be accounted for. In the proposed spring damper model, these properties are accounted for by m2.

Table 3. Effective masses of each thoracic impact and averages of effective masses according to appropriate modeling group: low speed lateral, low speed oblique, high speed lateral, or high speed oblique. Calculations of effective mass based on reports by Shaw et al 2006 and Matt Long.

	Effective Mass [kg]		
	Lateral		Oblique
Test			
503	18.5		22.7
504	37.7		36.6
505	27.2		27.1
506	29.9		29.1
507	23.7		26.2
601	25.7		28.3
602	34.2		34.9
Low Speed Average	28.1		29.3
802	36.1	803	36.7
902	42.3	804	34.2
903	18.2	901	31.1
High Speed Average	32.2		34.0

- K12 – K12 represents the spring stiffness of the subcutaneous tissue and fat as well as muscle located superficial to the skeletal ribs. It should be acknowledged that subcutaneous tissue is a very viscoelastic material that if studied alone would likely require a much more complicated model than a single spring. For this simulation, a simple spring model of tissue was initially selected because it was believed that the subcutaneous affects had minimal affects on the total thoracic deflection. This is believed to be the case since the subcutaneous tissue is a thin superficial membrane compared to thoracic spring damper components which are believed to dominate the total deflection of

the thorax. Initial estimate of spring stiffness of subcutaneous tissue was based on stiffness reported for Lobdell's anterior impact simulation.

- K23 – K23 represents the stiffness of the thoracic ribs. The effective mass of the ribs is accounted for in m2. The ribs are the primary support structure for the thorax. It is expected that the stiffness of the ribs will have a significant effect on simulated thoracic deflection.

- C23 – C23 represents the damping effects of the visceral components of the thorax. Visceral components of the thorax include any soft tissue contained within the thorax such as the heart and lungs. In addition, the thorax is a highly vascularized section of the body contained within the intercostals muscles attaching each rib superficially as well as the diaphragm inferiorly. When this thorax is impacted, blood contained within the vasculature of the thorax is forced to exit the thorax through the few vessels that exit the superior and inferior thorax. This affect has a significant damping affect which is accounted for with c23.

- Kve23 and Cve23 – It is well established that soft, biological tissues have significant viscoelastic properties. Viscoelastic material exhibit different deflection and shear stresses when loaded at different rates. Since this simulation of the thorax will include data from both low speed (2.5 m/s) and high speed (4.5 m/s) experiments,

inclusion of viscoelastic properties in thoracic model was deemed important in order to appropriately characterized deflection response of the thorax.

Simulations of total thoracic deflection and skeletal thoracic deflection will be performed with thoracic model. Definitions of total thoracic deflection and skeletal thoracic deflection are consistent with current definitions outlined in Ch 3. Total thoracic deflection is defined as the deflection of both the superficial, subcutaneous tissue and the deflection of the rib cage while skeletal deflection is defined solely as the deflection of the rib cage. As such, simulated total thoracic deflection will be defined as the difference between y1 and y3 while skeletal thoracic deflection will be defined as the difference between y2 and y3, Figure 13.

4.2 Model Parameters

Simulation of the thorax will be performed using the SimMechanics model of spring damper system outlined. In order for SimMechanics model to function, experimental data from thoracic impact testing will be used as an actuator to the system. Simulated results for total and skeletal thoracic deflection will be compared to experimental data of corresponding tests in order to calibrate and evaluate the thoracic deflection simulation. Profiles of input and output parameters for all three groupings experimental groupings can be seen in Appendix D.

4.2.1 Model Input Parameters

Actuation of the spring damper model will be performed by constraining the impactor mass (m1) to progress as if striking the thoracic model. Experimental potentiometer data from the impacting ram will be used to define the motion of the impactor. The SimMechanics model needs the position, velocity, and acceleration of the impacting mass in order to run a motion simulation based on experimental data. Velocity and acceleration of the ram are obtained through differentiation of the potentiometer data. Use of accelerometer data was considered as primary input to the model with velocity and position being the integral of the acceleration and double integral, but concern existed that accelerometer drift would overestimate the motion of the impacting ram. With the exception of parameters that are optimized in order to calibrate thoracic deflection, potentiometer data of ram motion is the sole model input into SimMechanics. All data from experimentation was filtered and prepared according to SAE J211 standards for biomechanical, automobile crash standards.

4.2.2 Model Output Parameters

As determined previously, primary evaluation of thoracic deflection simulation will be performed by comparing simulated thoracic deflection with experimental thoracic deflection. Calculations deriving total thoracic deflection will be based on data from the chestband placed around each surrogate at the level of the 4^{th} thoracic vertebra. However, since it is the hope that thoracic deflection simulation will be used as first step towards development of more biofidelic anthropometric measuring devices (ATDs), definition of total thoracic deflection must be consistent with deflection measurements based on geometry of current ATDs.

In current Anthropometric Measuring Devices (ATDs), the spine is where the majority of the ATD's thoracic mass is located which is defined as m3 in the current spring/damper model. Even when defining thoracic deflection in the lateral and oblique directions, m3 will still be associated with the spine. The "spine" section of ATD's is not similar to the spine section of the normal human. Spine sections are instead large masses that make up the remaining mass of the ATD in order to match the mass of the standard passenger. The spine section also acts as an attachment site for mechanical measurements (acceleration, deflection, etc.) and mechanical elements (springs and dampers) as it is the center of mass of the ATD's thorax. Since current definition of thoracic deflection based on chestband measurements is defined from the point of impact along the line of the ram's motion through to the opposite side of the thorax, the definition of thoracic

deflection defined in the model does not match results from the chestband measurements as they are used. Based on this observation, definition of thoracic deflection was redefined as half thoracic deflection.

Previous research defined the center of mass of the thoracic cavity as 44% of thoracic length from the spine to the sternum in the saggital plane[10]. Based on this definition, line of actuation for thoracic impact testing was defined as through the center of mass defined by this relationship for all experimental data obtained in thoracic impact testing. The definition of center of mass occurring at this point has been reused in order to define half thoracic deflections. Chestband data of projection of thoracic cavity in the transverse plane was reused in order to calculate thoracic half deflections. Vectors were defined as the distance between the spine position and the position of the sternum (V1) and distance between the spine and point of impact (V2). Distance vector between spine and sternum positions was multiplied by a factor of .44 in order to determine the center of mass (COM). Thoracic deflection was then redefined as the distance between the point of impact and the center of mass of the thorax calculated by determining the resulting vector between V2 and COM1, Figures 18 and 19.

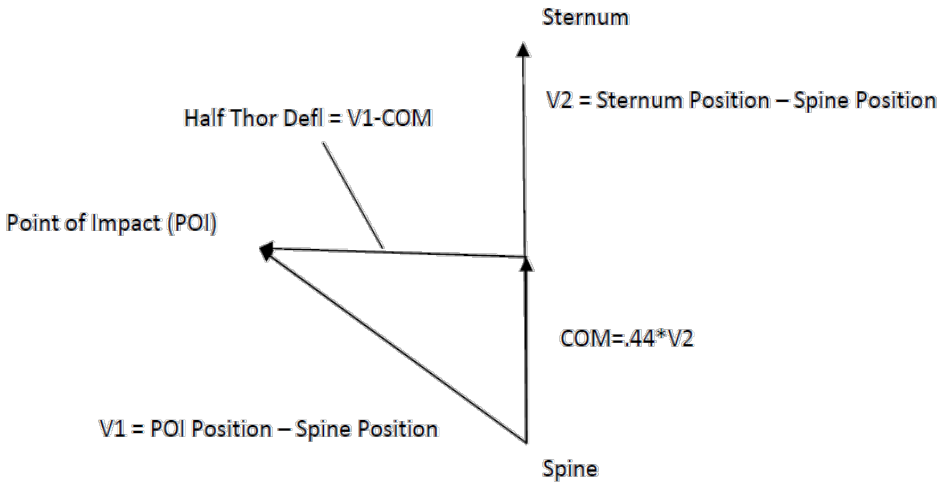

Figure 18. Definition of half thoracic deflection. Vectors used to define half thoracic deflection are based on position data of thoracic curvature as measured by chestband.

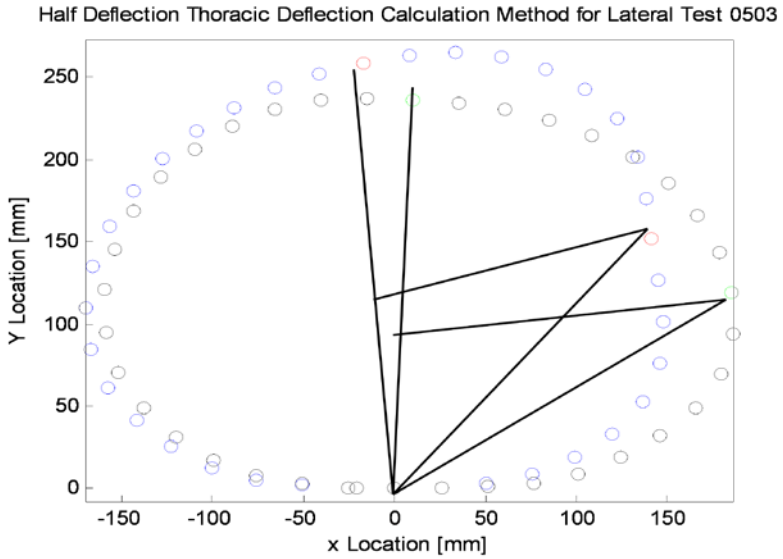

Figure 19. Example of definition of half thoracic deflection for left lateral thoracic impact experiment 0503. Black chestband contour shows initial position of thorax and blue chestband contour shows position of thoracic at maximum compression.

It is believed that this definition of thoracic deflection is the most accurate representation of deflections that ATDs measure that is presented by the experimental data. This definition of thoracic deflection will be used when comparing simulation thoracic deflection with experimental thoracic deflection.

The only other output from the SimMechanics thoracic simulation is force of thoracic impact. This quantity is evaluated by multiplying the mass of the impacting ram by the acceleration of the ram. Acceleration of the ram in the simulation was defined as the double derivative of the potentiometer data. This definition of ram acceleration was reused when calculating impact force.

4.3 Simulation Model Revisions

Lobdell's model of thoracic impact in the anterior direction was used as beginning point in development of SimMechanics simulation of thoracic deflection. Minor modifications to Lobdell's thoracic deflection model were performed in order to account for all factors that affect thoracic deflection. These revisions are outlined.

4.3.1 Impacting Ram Time of Contact

Observations of lateral and oblique stiffness curves shows significant irregularity for low speed impacts especially in the lateral impact orientation. Each lateral stiffness curve shows that the thorax absorbs significant loading with almost no deflection as

compared to oblique impacts which deflects approximately linearly with increased loading. Based on this observation, investigation into the experimental procedures of past thorax impact testing was conducted. Intuitively, lateral thoracic deflection curves do not make mechanical sense. The lateral stiffness curves based on the experimental data show that the thorax in the lateral direction remains extremely (if not infinitely) stiff during initial loading only to reach a breaking point where the thorax appears to deflect at a significantly different stiffness, Figure 20. These results only make sense if a major structural support of the thorax in the lateral direction is failing and the load is subsequently being absorbed by other structures. Since these tests are low speed and non-injurious impact scenarios, this is not the case.

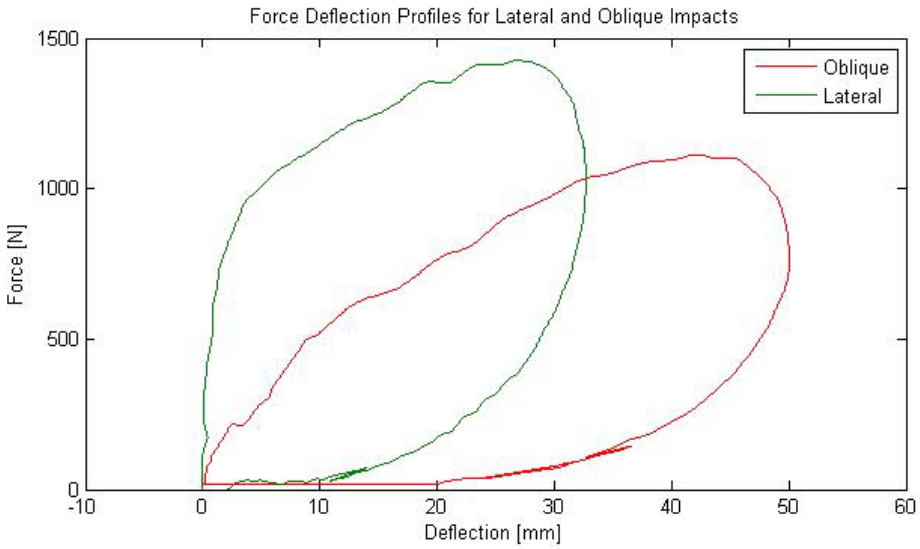

Figure 20. Average stiffness curves (force vs. deflection) for lateral and oblique impacts at low speeds (2.5 m/s). Observations show that lateral stiffness curve is highly irregular.

A review of low speed (2.5 m/s) test videos was conducted specifically for tests in the lateral direction. It was observed that the impact ram did not contact the lateral section of the thorax squarely , Figure 21. For several tests, it was observed that the superior section of ram impacted the surrogate prior to the center and inferior sections of the ram. Feducial markers are used to mark specific anatomical locations on the surrogate that are not easily visible. Feducas are yellow and black circles that can be seen in Figure 21. For the low speed tests, feducas were placed at the center of the impact ram as well as the thoracic level where the thoracic chestband was placed on the surrogate. It can be seen from the videos that at time zero, feducas marking the chestband position are noticeably inferior to the center of the impact ram.

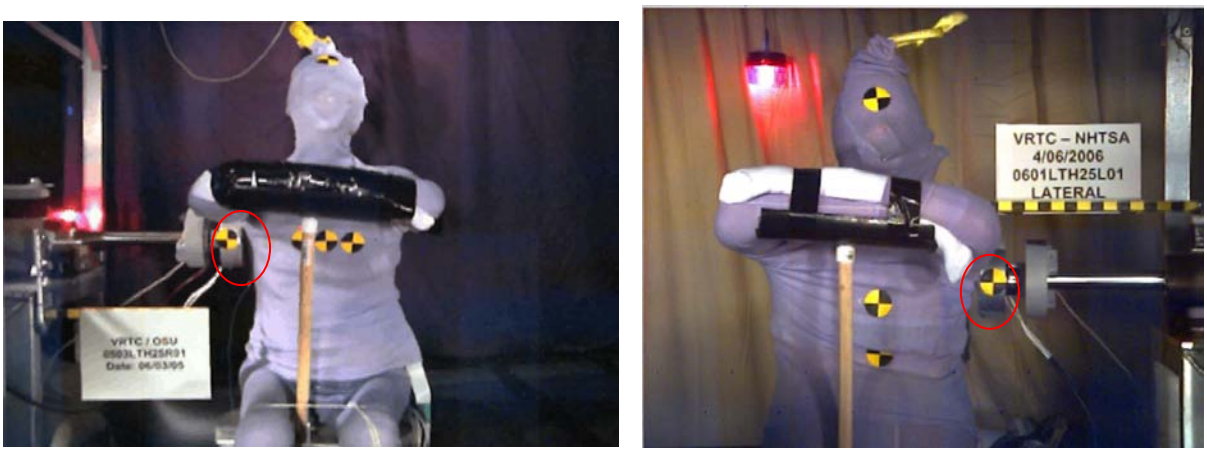

Figure 21. Stills of video recordings for lateral impact tests at time 0 seconds for two lateral impact tests. These tests were termed 0503 and 0601. Red circles highlight noticeable gap between inferior sections of ram and PMHS at time 0 seconds.

The combination of these two affects is believed to give an irregular shape to the lateral stiffness curves at low speeds. Initial loading is observed because of contact between the superior section of the ram with the thorax and/or shoulder of the surrogate. Minimal deflection is observed at this time because section of the thorax containing the chestband has not absorbed any loading. Chestband measurements only take into account deflections of the thorax at the level of the chestband. Any thoracic deflection outside of the cover of the chestband is not measured or accounted for. As such, simulation of thoracic deflection is a 2D simulation since the chestband data that is being used as a point of comparison only records the deflection of a transverse cross section of the thorax at the level of the 4^{th} thoracic vertebra.

In order to further prove that the ram was impacting solely the superior section of the thorax at time 0, moments from the load cell measuring force were reviewed, Figures 22 and 23. If loading was concentrated about the superior section of the thorax, it would be expected that a significant moment would be observed about the x-axis defined by the body coordinate system of the PMHS. Moments for all low speed (2.5 m/s) lateral tests were compared throughout the entire test. It was observed that tests labeled 0503 and 0601 had the largest moments about the x-axis which is consistent with observations from test videos.

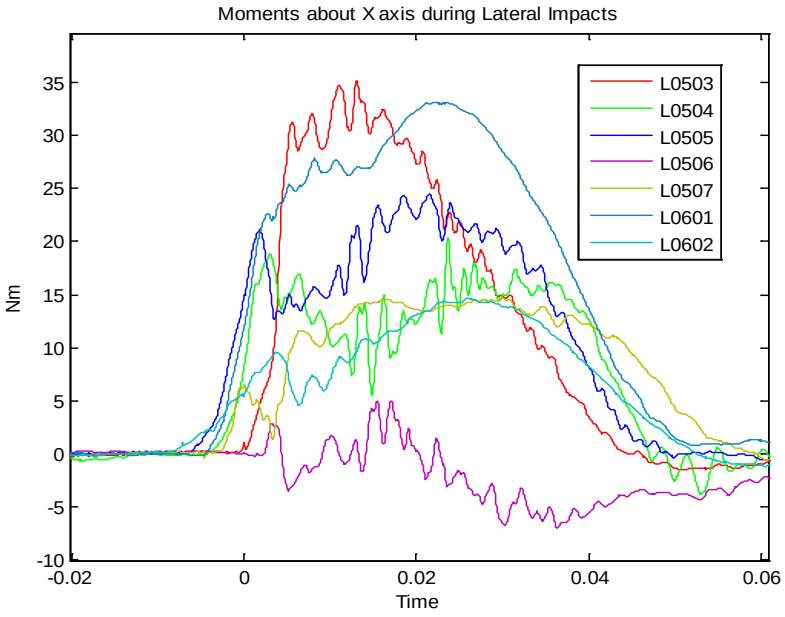

Figure 22. Moments about X-axis with respect to time for all 7 low speed (2.5 m/s) lateral impact tests.

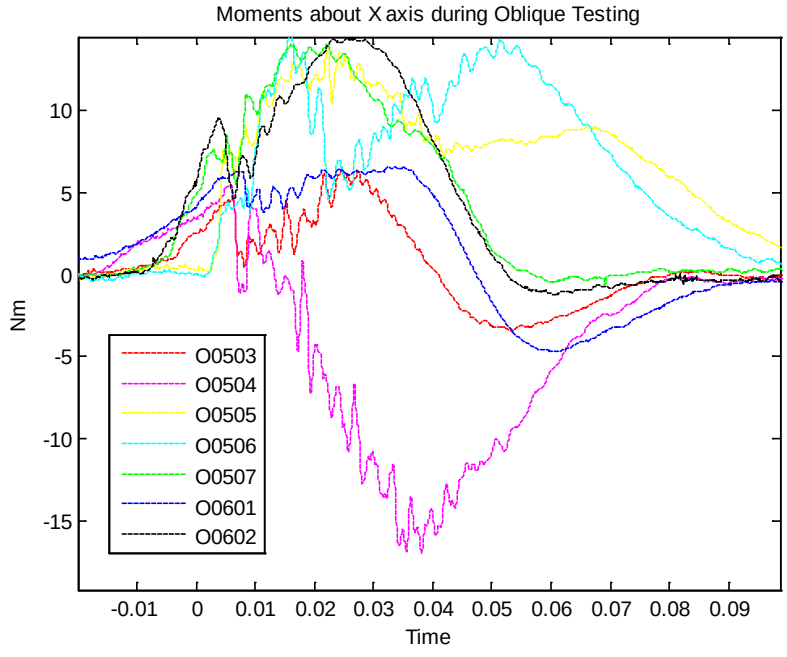

Figure 23. Moments about X-axis with respect to time for all 7 low speed (2.5 m/s) oblique impact tests.

Moments about the x-axis for oblique tests were reviewed in order to provide a point of comparison between lateral and oblique tests. The magnitude of moments about the x-axis for oblique low speed (2.5 m/s) test were observably smaller with maximum magnitudes approximately half as large as lateral tests. This confirms that different shapes of thoracic region of the body at lateral and oblique directions resulted in different loading profiles on the impactor ram. For lateral impacts, the force immediately following time 0 was concentrated on the superior sections of the pneumatic ram. Since the chestband only measures deflection along a narrow section of the thorax contained within the chestband, it is believe that delay in measurements of deflection is as a result of impact loading being concentrated at section of the thorax that did not contain the chestband. As ram continues to progress, entirety of ram face eventually makes contact with the thorax resulting in onset of measurable thoracic deflection.

Rough approximation of gap in between impacting ram and thorax at the level of the chestband can be approximated based on knowledge of approximately how fast the ram was traveling and time zero and the time delay between time zero and beginning of chestband measurements. Observations from figure 24 shows that onset of lateral deflection begins approximately 5 milliseconds after time 0. Based on these observations, gap between impacting ram and thorax at time zero is estimated to be 1.25 cm, which seems like a reasonable gap length considering the experimental test set up.

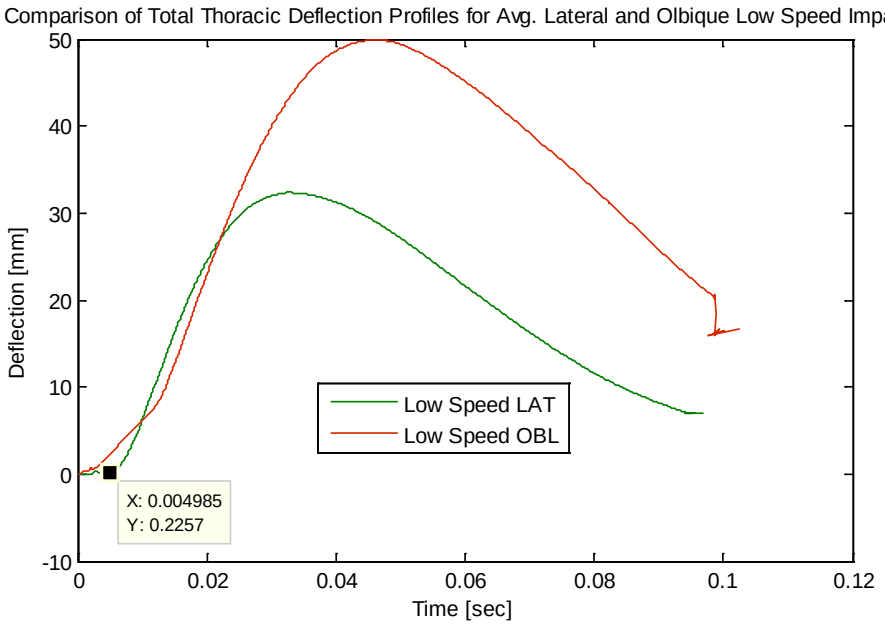

Figure 24. Comparison of average total thoracic deflection profiles for lateral and oblique low speed tests. Data cursor highlights point in time when thoracic deflection began for lateral impact experiments.

Observations from figure 24 also show that complications with chestband measurements are not isolated to solely the lateral impact orientation. For oblique impacts, chestband measurements of total thoracic deflection do begin at time zero. However, full onset of total thoracic deflection is delayed similarly to lateral impact experiments. Based on this observation, it is concluded that the complex geometries of the lateral and oblique impact sights influence the experimental deflection measurements of thoracic deflection as measured by the chestband. These influences need to be accounted for in the simulation of thoracic deflection. Since the majority of this influence is the result of a noticeable gap between the impacting ram and the thorax at time zero, a

defining parameter of the SimMechanics model of thoracic deflection will be a gap in between impacting ram and the skin section of the model. Methods for incorporating this feature into the SimMechanics model will be outlined.

4.4 SimMechanics Construction

A model of thoracic deflection was constructed in SimMechanics. Layout of SimMechanics model can be seen in Appendix B. SimMechanics model was generated using several Matlab SimMechanics functions within the Simulink toolbox. Some of these key features included: Body Blocks, In-Plane Joint Blocks, Joint Actuators, Spring and Damper Blocks, and Body Sensor Blocks. Body Blocks were used to simulate the mass sections of the spring damper model while Spring and Damper Blocks were used to simulate the springs and dampers in the spring damper model. In-Plane Joint Blocks constrained the motion of the body blocks to the x-y plane with actuation occurring solely in the y direction. A Joint Actuator Block was used to force the impact mass (m1) to move as constrained by experimental data from the potentiometer measurements taken during experimentation. Body Sensor Blocks recorded the position of each mass through time for calculations of total and skeletal thoracic deflection.

Since observations from experimental set up showed that cause of irregularity of stiffness profile was the result of a slight gap between the impactor and the thorax at the level of chestband placement at time zero (See ch 4.3.1), SimMechanics model was constructed in order to allow the impactor to travel freely for a given distance without compressing the thoracic section of the model. Length of distance that the impactor

traveled before compressing thorax was defined as another variable constant that could be adjusted similar to spring and damper coefficients. The methods for constructing such a SimMechanics model included modeling two impactors in SimMechanics. One is connected to the spring damper model just like previous versions of the thoracic model (real impactor) while the other impactor is unconstrained and allowed to move freely through space (dummy impactor). The simulation begins by actuating the dummy impactor and tracking its motion. When the dummy impactor has traveled a certain distance as defined by the user, the SimMechanics model allows the real impactor to actuate and forces it to move identically to the dummy impactor. As a result, the real impactor is only actuated after the ram has traveled a certain distance and accurately reflects what is observed from the real experimental set up. Preliminary testing of SimMechanics model set up showed that it was capable of generating stiffness curves similar to those observed in experimental data for low speed (2.5 m/s) impacts, Figure 25. Initial parameters used to develop these simulations were based on parameters used by Lobdell in his model of anterior thoracic deflections. It is believed with this adjustment of the spring damper model that the SimMechanics model now accurately reflects the experimental system.

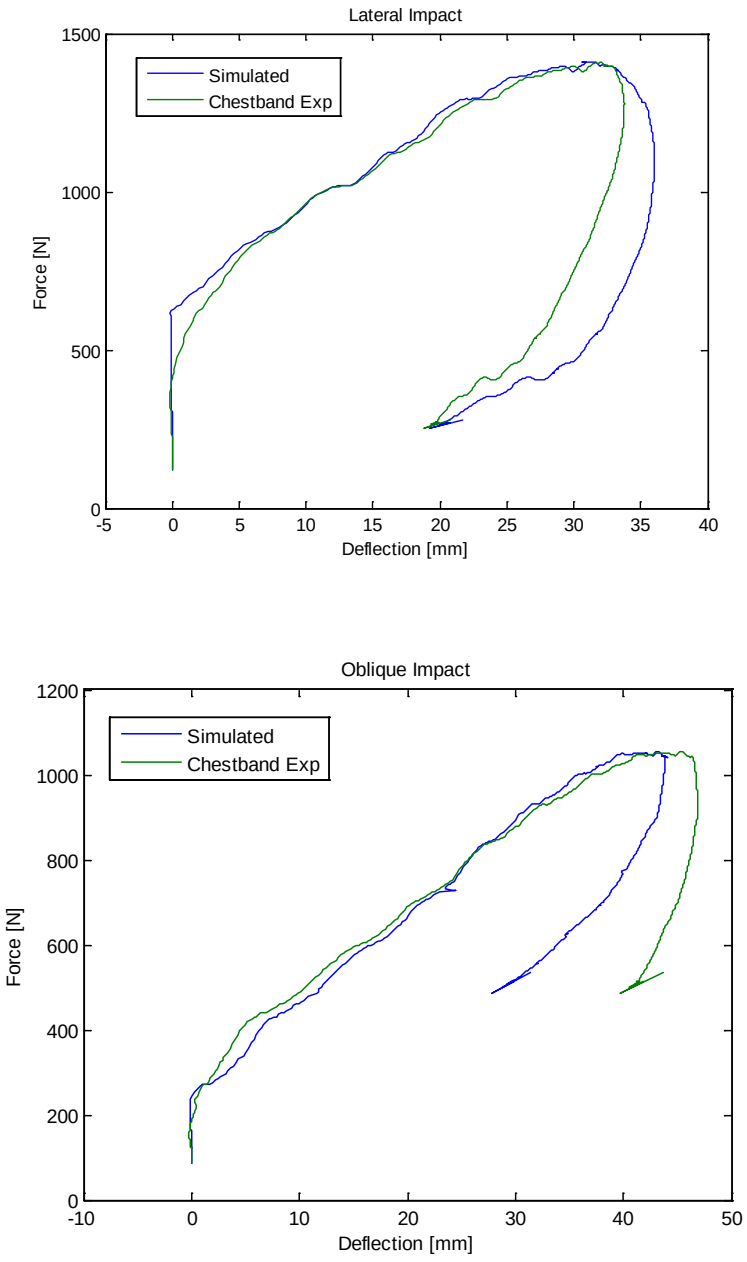

Figure 25. Comparison of experimental and simulated thoracic deflection for lateral (top) and oblique (bottom) impacts.

4.5 Summary

A SimMechanics model was developed to simulate thoracic deflection based on experimental data from thoracic impact experiments. SimMechanics model is based off spring damper model of thoracic deflection developed by Lobdell et al. Adjustments were made to Lobdell's model based on observations from experimental set up most notably the observable gap between the chestband and impacting ram at time zero. While SimMechanics model is able to replicated thoracic deflection responses similar in nature to those observed from experimental data, final value of spring and damper coefficients cannot be defined until optimization of thoracic model is complete. Optimization of thoracic model is outlined in Chapter 5.

CHAPTER 5

OPTIMIZATION METHODS AND RESULTS

In order to calibrate SimMechanics model to behave similarly to 50th percentile human thorax on impact, SimMechanics model was optimized comparing simulated to experimental thoracic deflection data. Methods of optimization and final results are outlined. Several optimization schemes were attempted in order to find the system model parameters that best match the 50th percentile human thorax. The final results from these optimizations schemes are outlined and discussed.

5.1 General Optimization Method

Optimization was performed using Optimtool, a function of Matlab. "Lsqcurvefit" function previously developed by Matlab was used as the optimization function. Matlab code was generated that performed simulation of SimMechanics model as outlined in Chapter 4 and can be seen in Appendix C. The final result of this Matlab code was the error between the simulated thoracic deflection and the experimental thoracic deflection as measured by the chestband, Equation 4. This function is the error function that Matlab is attempting to minimize.

$$error = def_{sim} - def_{\exp} \qquad (4)$$

In order to minimize this function Matlab was given control of six defining parameters of the thoracic simulation model. These parameters were m2, k23, c23, kv23, cv23, and delay. These parameters were the only parameters of the model that could not be calculated based on the experimental data or estimated based on previous research. The explanation of each these parameters is as follows:

- M2- M2 represents the inertial mass of the rib sections. The combined base of masses 2 and 3 was able to be calculated based on experimental data. The value of M2 was allowed to be fluctuated by Matlab code in order to determine the ratio between m2 and m3. M3 for the simulation will be calculated based on the difference between the thoracic effective mass and m2.
- K23, C23, KV23, and CV23- These are linear spring and damper constants that define the spring damper model. The reasoning for each the these springs/dampers was outlined in Chapter 4.1. There is no known way based on the experimental data that these constants could be approximated. K12 was assumed to be identical to the spring constant proposed by Lobdell during initial generation of this model.
- Delay- The delay parameter defines the distance between impactor and thorax at the plane of the chestband at time zero. This parameter was easily approximated. However, delay parameter was allowed to remain as an optimization parameter since the results of this parameter was not well understood and was initially believed to vary between lateral and oblique impacts.

The terminating command was either a normal difference in the optimization parameters or a normal change in the error function of less than .0001, whichever came first.

5.2 Initial Optimization Complications

It became apparent from initial optimization of low speed either lateral or oblique impacts that optimization solutions were not unique for each set of data. Lack of uniqueness was verified by running optimization multiple times under different false constraints. For the first optimization, lateral impact simulation was optimized relative to lateral impact experimental data. For this optimization scheme, Matlab optimization was allowed to solve the optimization problem to whichever parameters values it chose.

Alternatively, optimization problem was rerun with minor modification: a single parameter from the optimization problem was forced to be a certain value. Under this initial constraint, Matlab optimization solved the problem to a separate solution with equivalent goodness of fit to the original solution, Figure 26). These results showed that original Matlab optimization scheme was not generating unique solutions. Instead, infinity many solutions exist to the optimization which makes it impossible to determine which solutions actually represent reality. As a result, it becomes impossible to draw conclusions from the simulation. When optimization problems have such conclusions, two solutions exist to redeem problem: simplify initial model or include additional data to better define the system. Both of these methods were attempted in varying ways order to determine unique solution to the optimization problem.

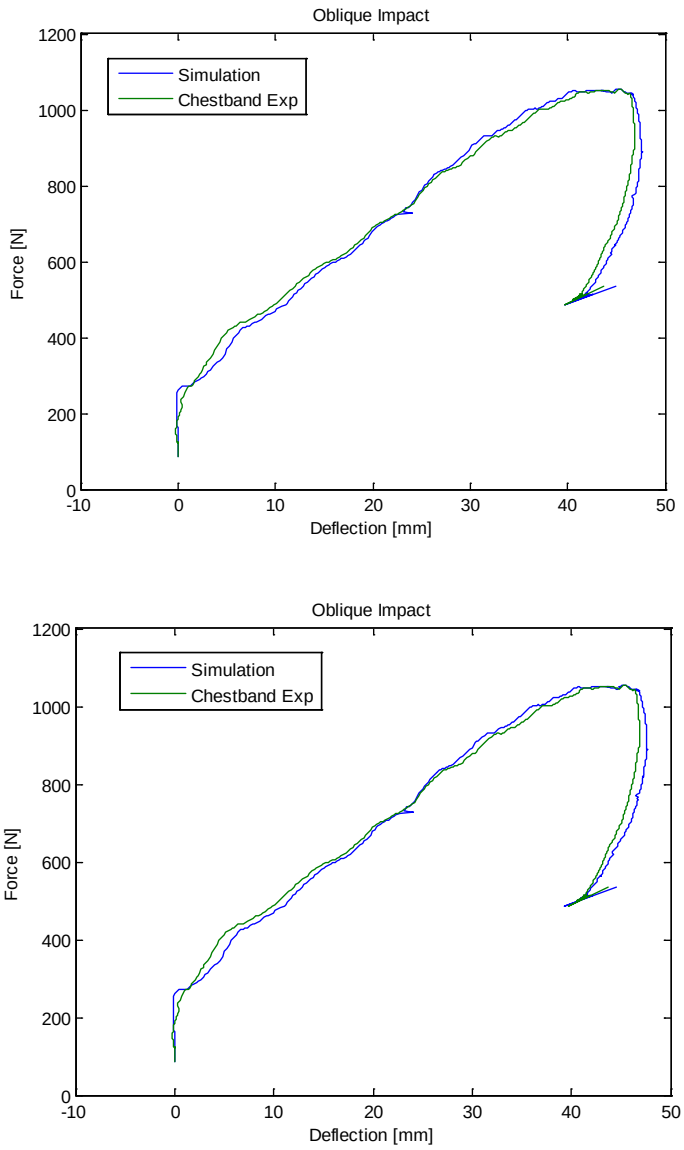

Figure 26. Comparison of different oblique impact optimization solutions. Stiffness profiles represent different goodness of fits despite having completely different input parameters. Unconstrained solution (top) was initially determined by Matlab. Falsely constrained solution (bottom) defined kv23 as 3000 and observed different solution to optimization problem.

5.3 Attempted Optimization Schemes

In order to account for non-uniqueness of initial optimization problem solutions, several optimization schemes were attempted with varying success. Optimization schemes attempted to either simplify the initial model or incorporate additional constraints from other experimental data points. Numerical values to each solution can be observed in Table 4.

5.3.1 Optimization Scheme 1-High Speed and Low Speed Simultaneous Optimization

With the recent completion of high speed impacts (4.5 m/s) within the IBRL, initial proposal to determine unique solution to thoracic model was to optimize the model to both low speed (2.5 m/s) and high speed (4.5 m/s) experimental data at the same time for either lateral and oblique impacts. It was the hope that optimizing each impact orientation to both high speed and low speed data would better define the experimental system being simulated and eliminate optimization solutions that do not accurately represent reality. The best solution to this optimization problem can be observed in Figure 27. The unexpected result showed that the model intended to simulate thoracic deflection for low speed data did not result in good approximations of high speed impact data.

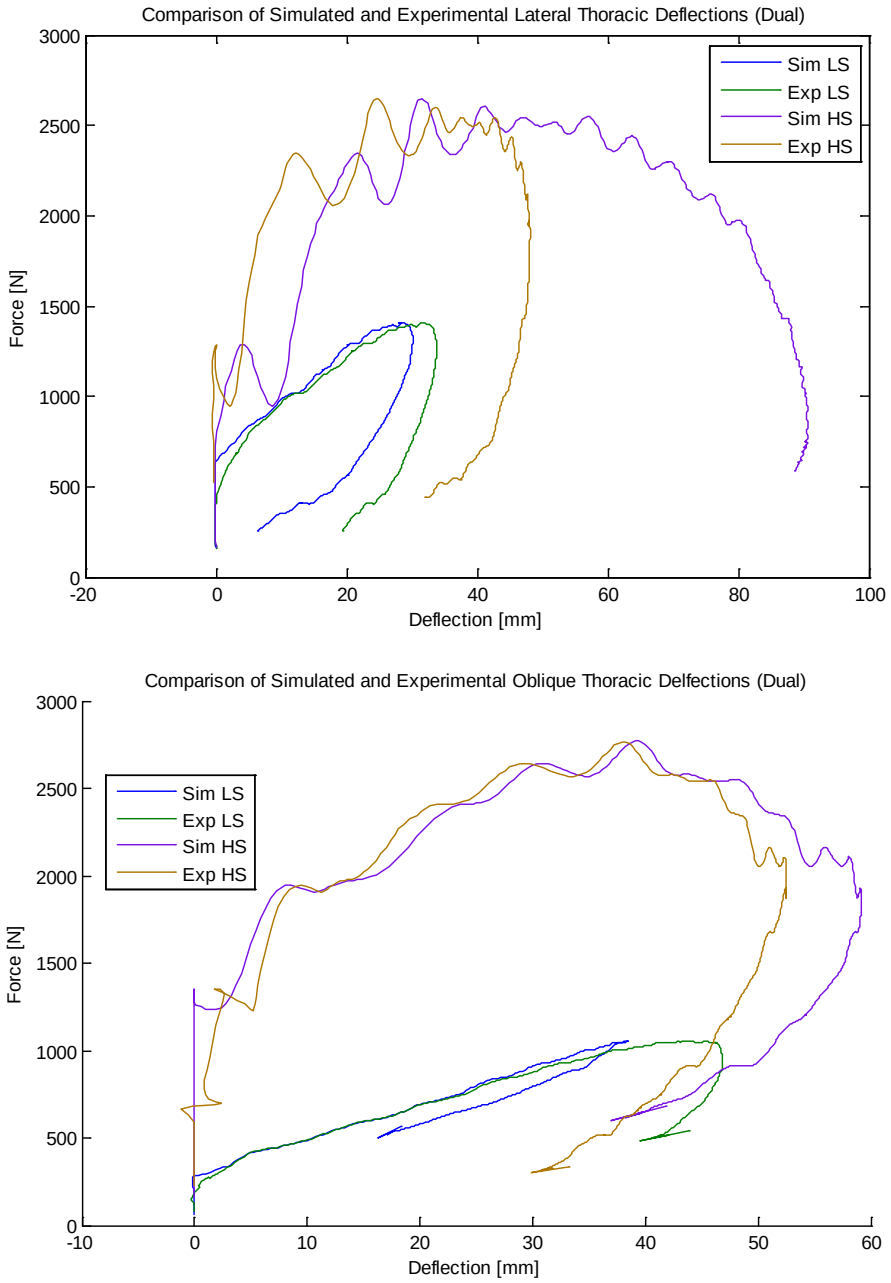

Figure 27. Comparison of simulated and experimental thoracic deflection for lateral (top) and oblique (bottom) impact orientations under optimization scheme 1. Optimization scheme one optimized the model to both low speed and high speed impact experimental data.

especially in the lateral impact orientation. As can be observed in Figure 27, simulate significantly overestimates thoracic deflection compared to experimental data for lateral impact orientation. For oblique impact orientations, final solution does not fit low speed well. Oblique low speed simulation underestimates thoracic deflection.

With the previously observed quality of fit for low speed impact, inability of optimizer to obtain solution that matched low and high speed experimental data for each impact orientation was either the result of the model's inability to generate a response similar to high speed experimental data or that no solution existed that matched low and high speed data. In order to determine which case was present in the current simulation, the model was optimized solely to high speed experimental data in the lateral impact orientation. Results from this optimization problem showed that SimMechanics model of thoracic deflection was unable to match experimental data for thoracic deflection under high speed lateral impact orientation. Optimization of parameters for solely the high speed lateral impact configuration resulted in simulated thoracic deflection that overestimated total thoracic deflection as previously observed, Figure 28.

5.3.2 Optimization Scheme 2-Low Speed Lateral and Oblique Simultaneous Optimization

With the model's observed inability to simulate thoracic deflection, focus was shifted back to low speed tests in both the lateral and oblique orientations which was the initial scope of research project. It was assumed that lateral and oblique impact

orientations had mechanical properties that were approximately similar in there majority with only slight differences that account for the differences observed experimentally.

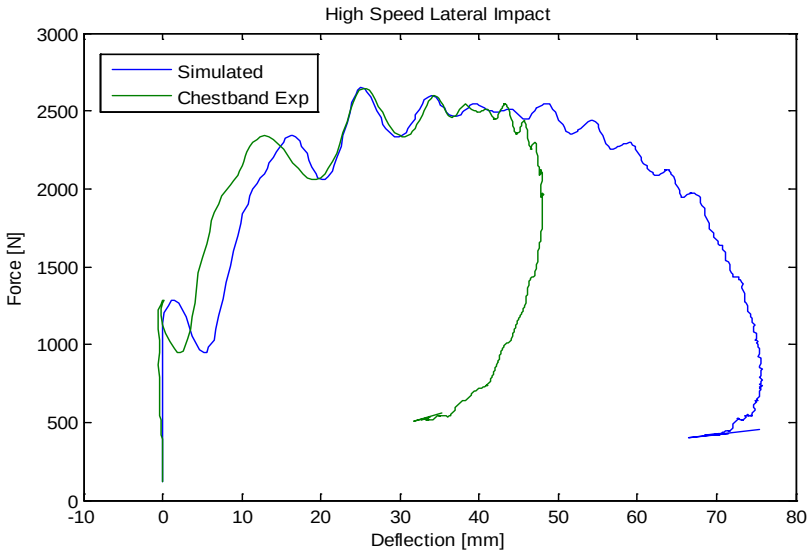

Figure 28. Comparison of simulated and experimental thoracic deflection for lateral high speed thoracic impact for solution to optimization problem that focused only on high speed lateral impact.

This was believed to be the case since both impact orientations share the majority of similar structures. Based on this assumption, optimization scheme was developed that optimized low speed impact thoracic model to lateral and oblique impact orientations in order to find the solution that provided a best fit to both impact orientations. This solution would be reused as an initial estimate in an alternative optimization problem that focused on either the lateral or the oblique low speed impact configurations. It was the belief that using this dual optimization of both low speed impact orientations would drive the final optimization towards a solution that was constrained by both lateral and oblique impact orientations in order to eliminate false solutions in either the lateral or oblique impact

orientations. Optimization of both lateral and oblique low speed impact compared to experimental data can be seen in figure 29.

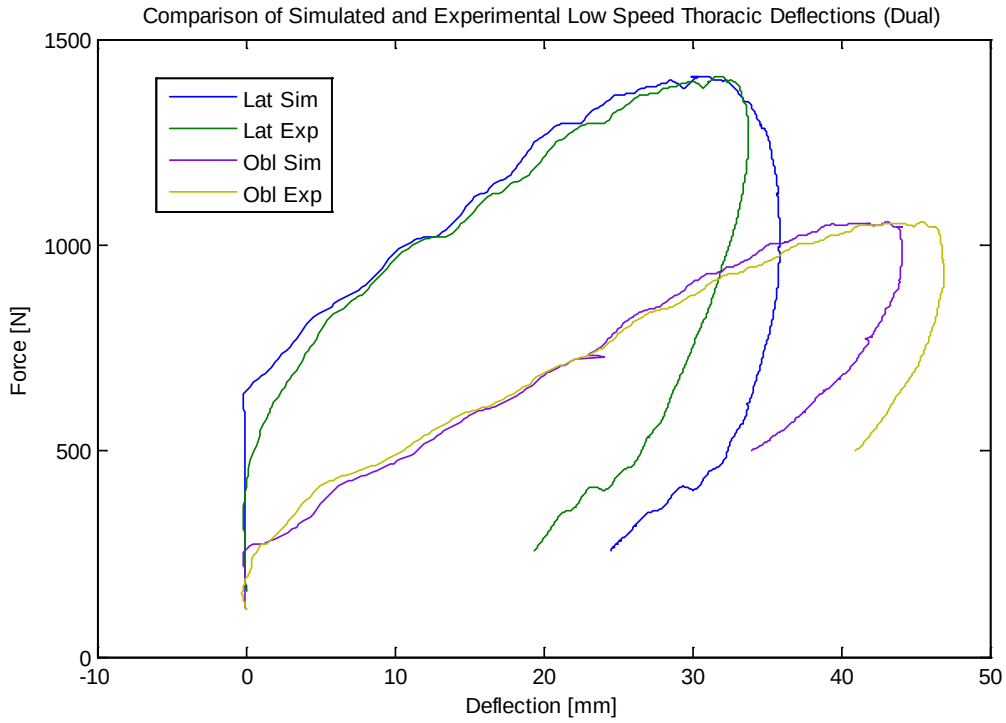

Figure 29. Comparison of simulated and experimental thoracic deflection for lateral and oblique low speed impacts for optimization problem when lateral and oblique low speed impacts were optimized together.

Based on observed results from this optimization scheme, dual optimization for low speed data leads to reasonable simulations in both the lateral and oblique impact orientations when using the same parameters to define the mechanical aspects of the thorax. The only major deviations between the lateral and oblique low speed simulated and experimental thoracic deflections was observed in the rebound of the thorax after

maximum deflection was already reached. This section of the stiffness curve is less important than response of the thorax to initial loading.

5.4 Discussion of Best Approximation

The thoracic deflection model's inability to simulate thoracic response for the high speed data makes conclusion of model parameters impossible since lack of data that is able to be modeled exists. However, optimizing low speed lateral and oblique simulations to experimental data dually provided interesting results. This optimization scheme shows that optimization solution based on spring damper model can result in a decent approximation of both lateral and oblique impacts for the low speed impact velocity using the same model parameters. This result shows that lateral and oblique impact orientations for the low speed impact velocity are not as different as initially thought based on varying stiffness curves. Although slight difference between the lateral and oblique orientations are apparent from the optimization/s inability to find a solution that better fits the experimental data for both orientations, the internal mechanical structures of the thorax have very similar magnitudes of resistance. These simulation results in addition with the similarly in lateral and oblique impact orientations observed for high speed impacts show that despite initial low speed impact finding, it may still be possible that internal mechanical response of thorax to lateral and oblique impact orientations are equivalent when observing total thoracic deflection.

Table 4. Optimized parameters for each optimization scheme.

		m1 [kg]	k23 [N/m]	c23 [Ns/m]	kv23 [N/m]	cv23 [Ns/m]	delay [m]
Low and High Speed Opt	Lateral	0.102	84.7	1200	1575	2284	0.013
	Oblique	0.102	68.8	1241	1301	2428	0.013
Lateral and Olbique Opt	Low Speed Data	0.210	2767	490	4172	3652	0.013

Optimized parameters for both optimization schemes can be seen in table 4. Unfortunately, several parameters for both optimization schemes do not correspond well to each other which would have provided addition support to the construction of the thoracic model. This is believed to be because of the model's inability of simulate the high speed impact data. This results makes the parameters from scheme 1 less trustworthy which does not allow for easy comparison.

5.5 Summary

Optimization methods used to generate thoracic response similar to experimental data for lateral and oblique high and low speed data are outlined. Optimization of low speed model in the lateral and oblique directions was impossible since multiple solutions existed to the optimization problem in both orientations. Optimization methods were performed against high speed impact data for lateral and oblique impact orientations and it was observed that current model was unable to simulate thoracic deflection in the lateral and oblique directions with most significant errors for the high speed lateral impact orientation. These observations made firm conclusions from the model based on current data sets impossible. It was observed that when optimization was performed with low speed lateral and oblique data at the same time that a reasonable solution to the optimization problem did exist. This provides the opportunity that lateral and oblique

internal responses to impact for the low speed data are similar despite observed differences from initial experimental findings.

CHAPTER 6

FUTURE WORK AND CONCLUSION

The total results of this research project show that the thoracic response to impact in the lateral and oblique directions is still not well enough understood to generate accurate simulations based on methods outlined. However, the importance of a better understanding of the directional dependence of the thoracic response is emphasized. When performing motion analysis of accelerometer arrays placed on the rib sections during low speed thoracic impacts, Chapter 3, it was consistently observed that skeletal deflection was greater in the oblique impact orientation and that larger percentages of the total thoracic deflection were absorbed by the soft tissue covering the skeletal structure of the thorax in the lateral impact orientation. Since larger deflections of the skeletal structure of the thorax will result in greater injury to the ribs and deeper structures of the thorax, the importance of understanding the oblique and other orientations is emphasized as these results imply that greater injury may be observed at this orientation for similar loadings.

Results from optimization show that the system is not well enough defined with current experimental data in order to accurately simulate thoracic response or the experimental data is not well simulated by the model proposed. Alterations of the model

or factors not considered that influence the mechanical response of the thorax need to be investigated in order to develop a better understanding of the thoracic response at high speeds. This is of particular importance since it is at these speeds that severe injury is actually observed in real life traffic collisions. Recent suggestions were made based on observed inability of high speed model to simulate thoracic response to correct for these complications. These suggestions included accounting for the varying effective mass of the thorax and including non linear springs/dampers. These options were not explored in this thesis due to lack of time and may be investigated at a later time based on initial research into validity of possibility. Additionally, assumption that skin stiffness (k12) could be approximated based on value use by Lobdell identically for lateral and oblique impacts needs to be evaluated. Since motion simulation showed that greater soft tissue deflection was observed in the lateral impact orientation, this implies that skin stiffness value used in the model may need to vary between lateral and oblique impacts. This would most easily be done by including it as an optimization parameter.

Finally and most importantly, the results from the optimization of lateral and oblique low speed experimental results simultaneously show that current simulation is able to generate approximate fits of the experimental data with the exact same input parameters. This result allows for the potential that the lateral and oblique low speed responses are more similar than initially thought with only minor mechanical differences for the two impact orientations, at least in the internal response. It was observed in ch 4 that the loading profiles on the thorax for low speed impacts in the lateral and oblique directions showed significant variation. It is not outside of the possibility that observed

differences in the thoracic response were the result of external biomechanical influences such as thorax/ ram contacting geometry and stability of the seated position of the PMHS at the point of impact. It is impossible to determine based on the analysis completed whether this is the case, but should be considered more closely as part of future work investigating the thoracic response.

BIBLIOGRAPHY

1. Stapp Car Crash Conference. Pp. 35-53. Society of Automotive Engineers, Warrendale, PA. Eppinger, R. (1979) Prediction of thoracic injury using measurable experimental parameters.

2. Eppinger, R., Marcus, J. and Morgan, R. (1984) Development of dummy and injury index for NHTSA's thoracic side impact protection program. Proc. SAE Government/Industry Meeting. Pp 983-1011. Society of Automotive Engineers, Warrendale, PA.

3. Eppinger, R. (1989) On the development of a deformation measurement system and its application toward developing mechanically based injury indices. 33rd Stapp Car Crash Conference. Pp. 21-28. Society of Automotive Engineers, Warrendale, PA.

4. Federal Register, Volume 55. (1990) Rules and Regulations. U.S. Government, Washington, D.C. ISO/TR9790(E). (1999) Road vehicles –Anthropomorphic Side Impact Dummy – Lateral Impact Response Requirements to Assess the Biofidelity of the Dummy. ISO/DTR 9790-7 Document N455 – Revision E.

5. Kroell, C., Schneider, D., and Nahum, A. (1971) Impact tolerance and response of the human thorax. 15th Stapp Car Crash Conference. Pp 84- 154. Society of Automotive Engineers, Warrendale, PA.

6. Kroell, C., Schneider, D., and Nahum, A. (1974) Impact tolerance and response of the human thorax II. 18th Stapp Car Crash Conference. Pp 383-457. Society of Automotive Engineers, Warrendale, PA.

7. Neathery, R., and Lobdell, T. (1973) Mechanical simulation of human thorax under impact. 17^{t}Stapp Car Crash Conference. Pp 451-466. Society of Automotive Engineers, Warrendale, PA.

8. Pintar, F., Yoganandan, N., Hines, M., Maltese, M., McFadden, J., Saul, R., Eppinger, R., Khaewpong, N., and Kleinberger, M.. (1997) Chestband analysis of human tolerance to side impact. 41^{sst} Stapp Car Crash Conference. Pp. 63-74. Society of Automotive Engineers, Warrendale, PA.

9. Viano, D. (1989) Biomechanical responses and injuries to blunt lateral impact. 33rd Stapp Car Crash Conference. Pp 113-142. Society of Automotive Engineers, Warrendale, PA.

10. Shaw J.M., Herriott R. G., Donelly B.R., McFadden J.D., Bolte J.H. (2006) Oblique and Lateral Response of the PMHS Thorax. 50th Stapp Car Crash Conference. pp. 147-167. Society of Automotive Engineers, Warrendale, PA.

11. Net Anatomy accessed on May 18th 2010.
Image Source: http://www.netanatomy.com/bobCSA/csa_frame.asp

Appendix A—Results of Adams View Motion Analysis and Equivalent Chestband Modeling

Experiment 0503—

Chestband	Lateral	Oblique
Max Compression (mm)	31.5	56.4
Initial Chest Depth (mm)	345.1	326.8
Gauge 1	16	8
Gauge 2	35	26
Number of Gauges	37	37
Time of Max Compression (sec)	0.029	0.037
Percent Compression (%)	9.1%	17.3%

Adams	Lateral	Oblique
Max Compression (mm)	NA	46.4
Initial Chest Depth (mm)	NA	297
Gauge 1	RLat	LAnt
Gauge 2	LLat	RPos
Time of Max Compression (sec)	NA	0.045
Percent Compression (%)	NA	15.6%

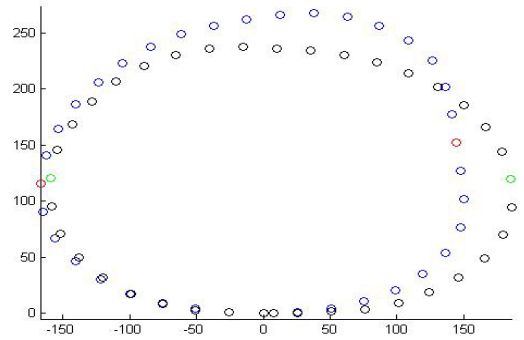

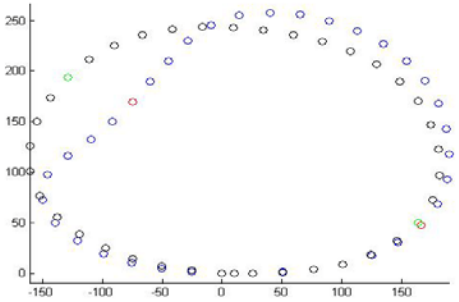

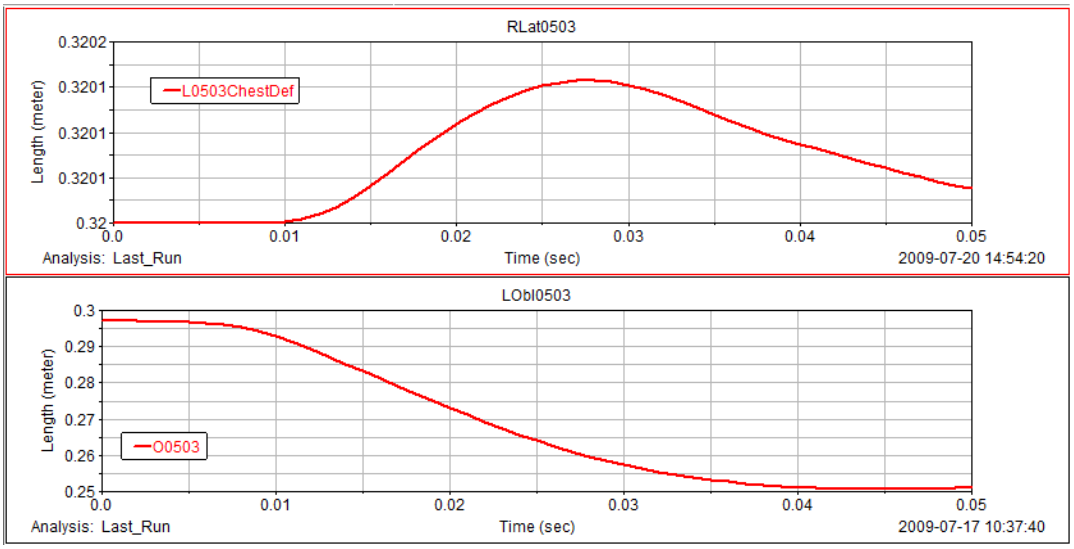

Experiment 0504—

Chestband	Lateral	Oblique
Max Compression (mm)	40.0	44.9
Initial Chest Depth (mm)	399.4	382.4
Gauge 1	11	9
Gauge 2	33	30
Number of Gauges	40	40
Time of Max Compression (sec)	0.035	0.041
Percent Compression (%)	10.0%	11.7%

Adams	Lateral	Oblique
Max Compression (mm)	8.2	29.1
Initial Chest Depth (mm)	365	320
Gauge 1	LLat	Rant
Gauge 2	RLat	Lpos
Time of Max Compression (sec)	0.037	0.038
Percent Compression (%)	2.2%	9.1%

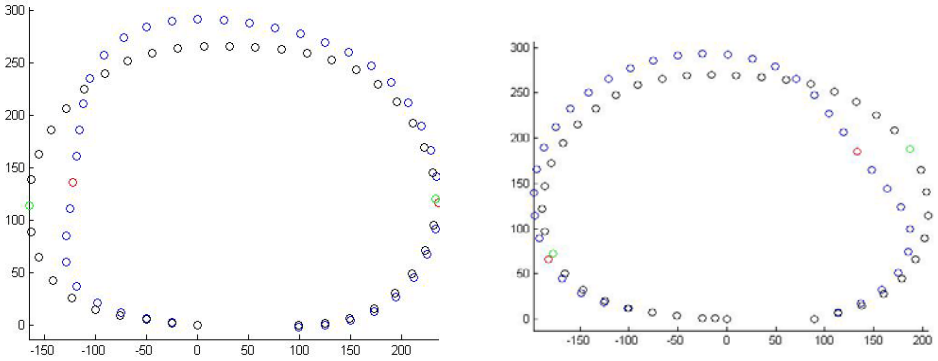

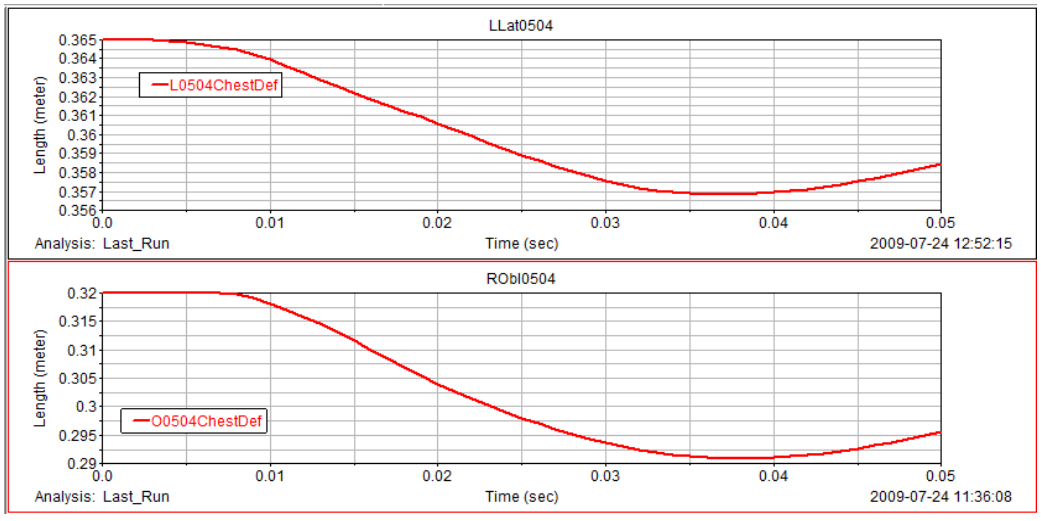

Experiment 0505—

Chestband	Lateral	Oblique
Max Compression (mm)	34.1	64.7
Initial Chest Depth (mm)	339.9	324.5
Gauge 1	8	16
Gauge 2	28	36
Number of Gauges	39	39
Time of Max Compression (sec)	0.029	0.055
Percent Compression (%)	10.0%	19.9%

Adams	Lateral	Oblique
Max Compression (mm)	14.8	54.4
Initial Chest Depth (mm)	320	300
Gauge 1	RLat	Lant
Gauge 2	LLat	Rpos
Time of Max Compression (sec)	0.034	0.05
Percent Compression (%)	4.6%	18.1%

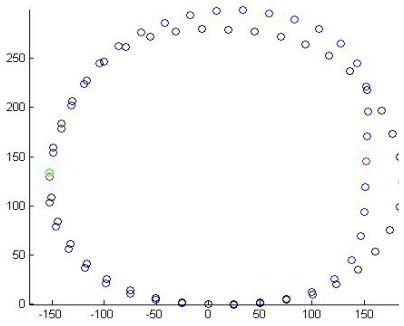

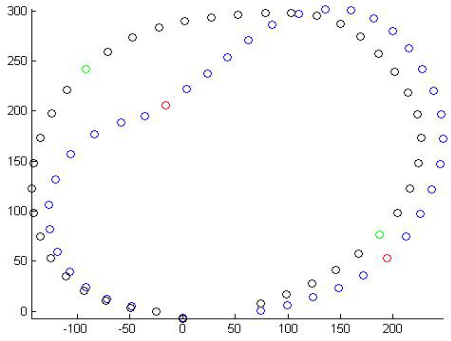

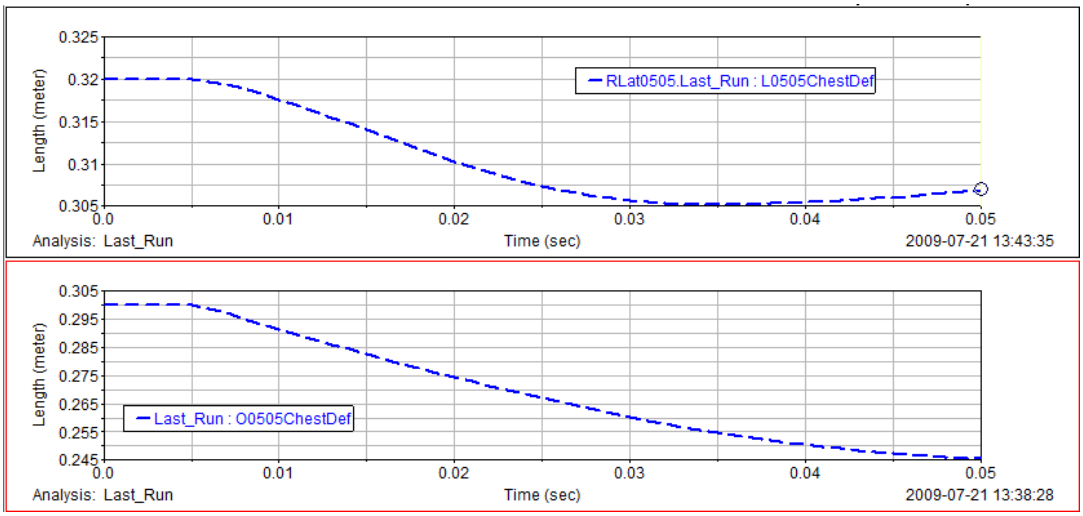

Experiment 0506—

Chestband	Lateral	Oblique
Max Compression (mm)	30.5	51.9
Initial Chest Depth (mm)	347.6	345.2
Gauge 1	10	11
Gauge 2	28	30
Number of Gauges	35	37
Time of Max Compression (sec)	0.029	0.041
Percent Compression (%)	8.8%	15.0%

Adams	Lateral	Oblique
Max Compression (mm)	10.2	47.5
Initial Chest Depth (mm)	328	298
Gauge 1	LLat	Rant
Gauge 2	RLat	Lpos
Time of Max Compression (sec)	0.038	0.043
Percent Compression (%)	3.1%	15.9%

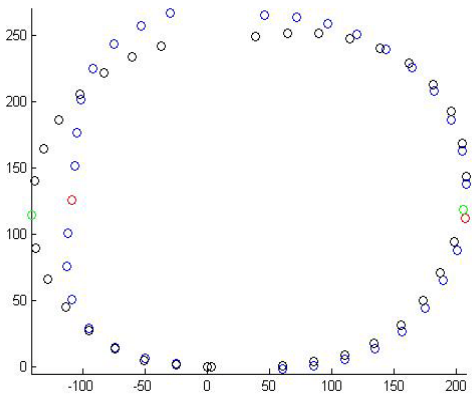

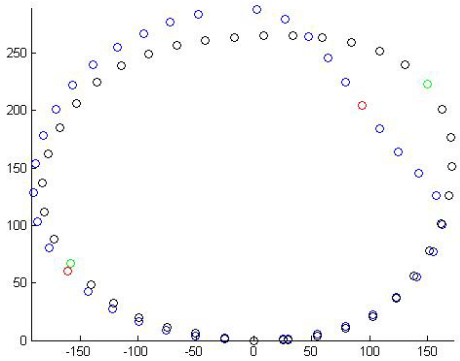

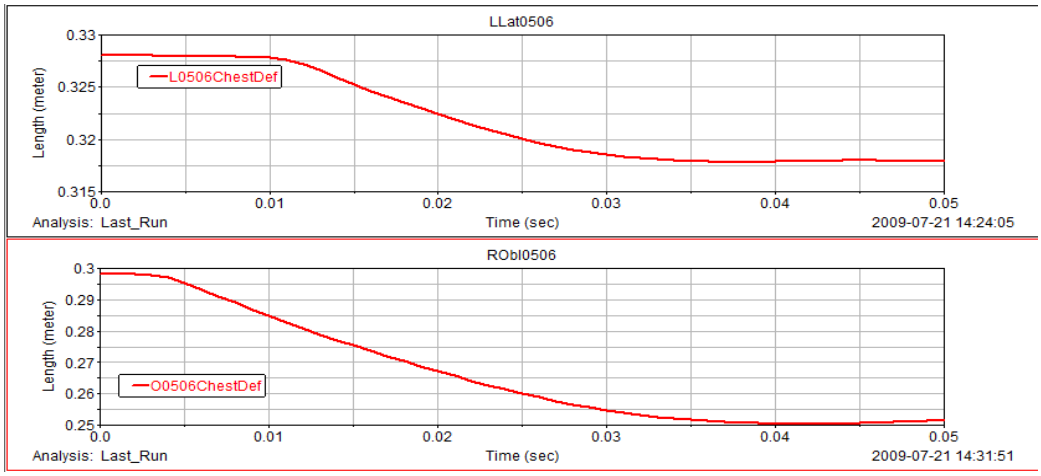

Experiment 0507—

Chestband	Lateral	Oblique
Max Compression (mm)	44.7	52.3
Initial Chest Depth (mm)	342.6	328.5
Gauge 1	6	16
Gauge 2	26	36
Number of Gauges	40	40
Time of Max Compression (sec)	0.031	0.039
Percent Compression (%)	13.0%	15.9%

Adams	Lateral	Oblique
Max Compression (mm)	22.9	37.2
Initial Chest Depth (mm)	311	301
Gauge 1	RLat	Lant
Gauge 2	LLat	Rpos
Time of Max Compression (sec)	0.037	0.050
Percent Compression (%)	7.4%	12.4%

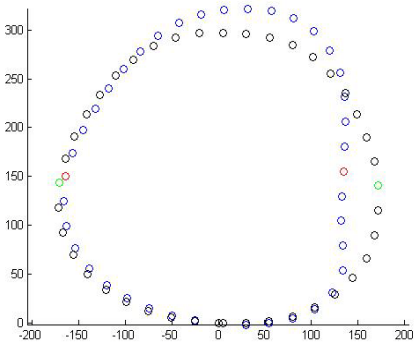

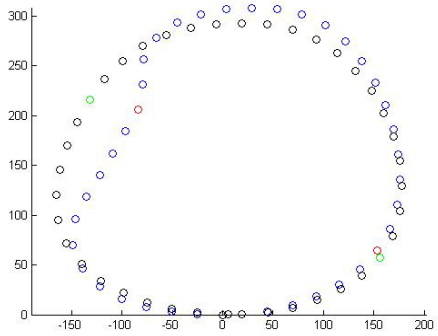

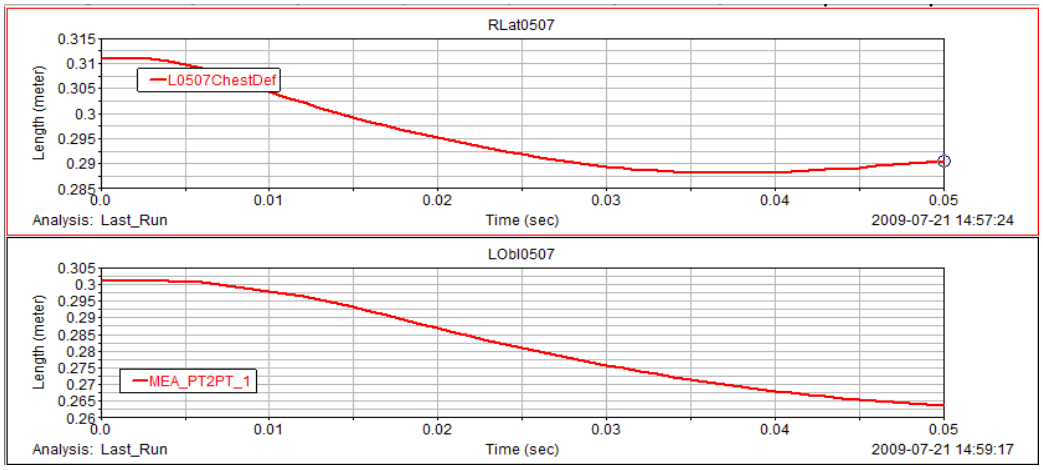

Experiment 0601—

Chestband	Lateral	Oblique
Max Compression (mm)	34.4	49.1
Initial Chest Depth (mm)	329.4	325.3
Gauge 1	12	18
Gauge 2	31	38
Number of Gauges	40	40
Time of Max Compression (sec)	0.029	0.047
Percent Compression (%)	10.4%	15.1%

Adams	Lateral	Oblique
Max Compression (mm)	15	23.7
Initial Chest Depth (mm)	363	346
Gauge 1	LLat	Rant
Gauge 2	RLat	Lpos
Time of Max Compression (sec)	0.030	0.042
Percent Compression (%)	4.1%	6.8%

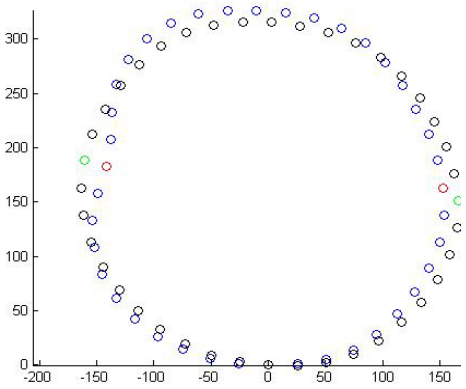

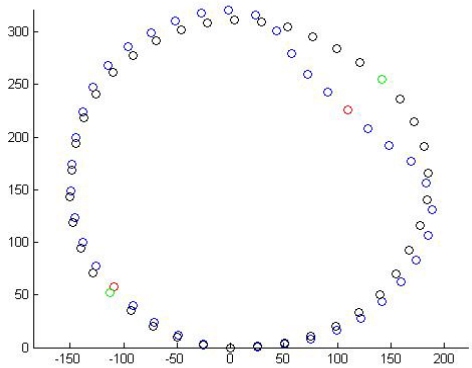

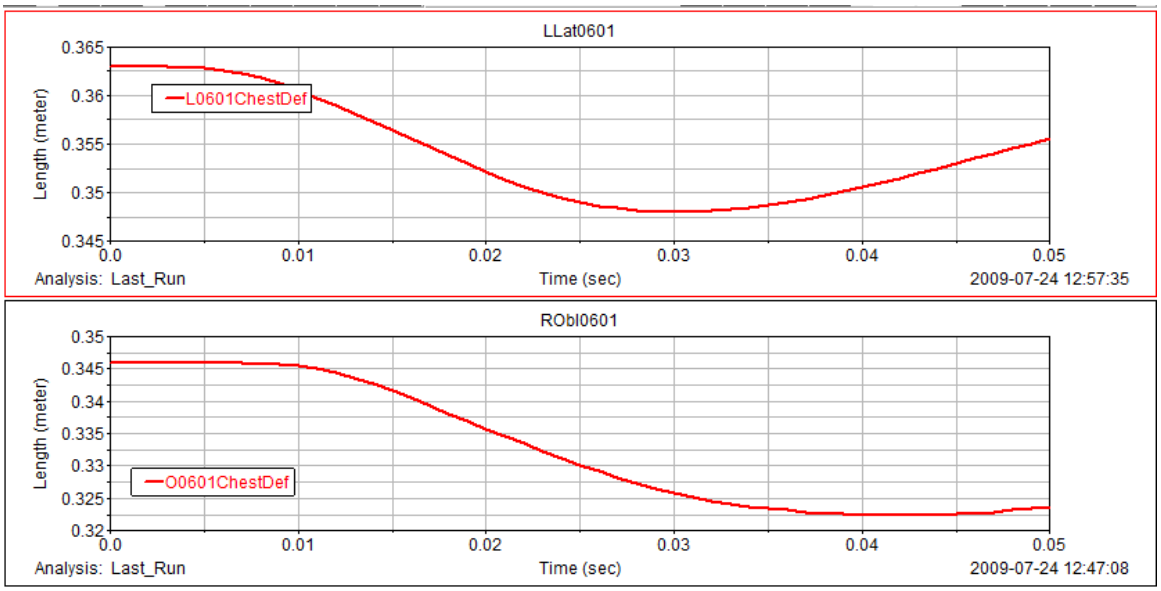

Experiment 0602—

Chestband	Lateral	Oblique
Max Compression (mm)	68.3	44.9
Initial Chest Depth (mm)	369.6	338.4
Gauge 1	5	16
Gauge 2	25	36
Number of Gauges	40	40
Time of Max Compression (sec)	0.029	0.047
Percent Compression (%)	18.5%	13.3%

Adams	Lateral	Oblique
Max Compression (mm)	15.6	31.7
Initial Chest Depth (mm)	349	334
Gauge 1	RLat	LAnt
Gauge 2	LLat	RPos
Time of Max Compression (sec)	0.033	0.043
Percent Compression (%)	4.5%	9.5%

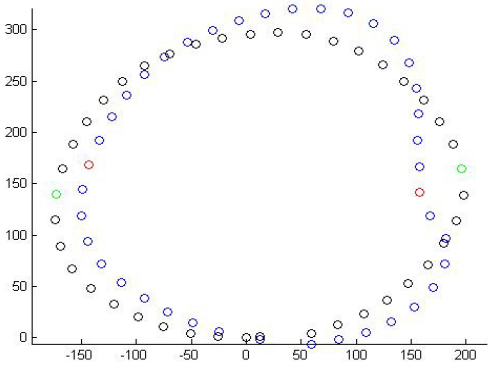
300
250
200
150
100
50
0
-150
-100
-50
0
50
100
150
200

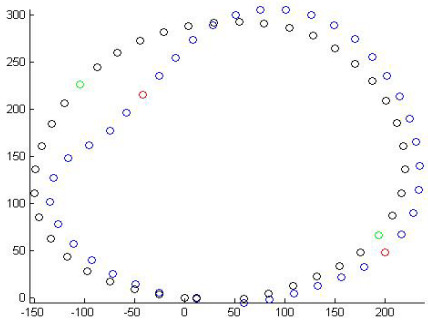
300
250
200
150
100
50
0
-150
-100
-50
0
50
100
150
200

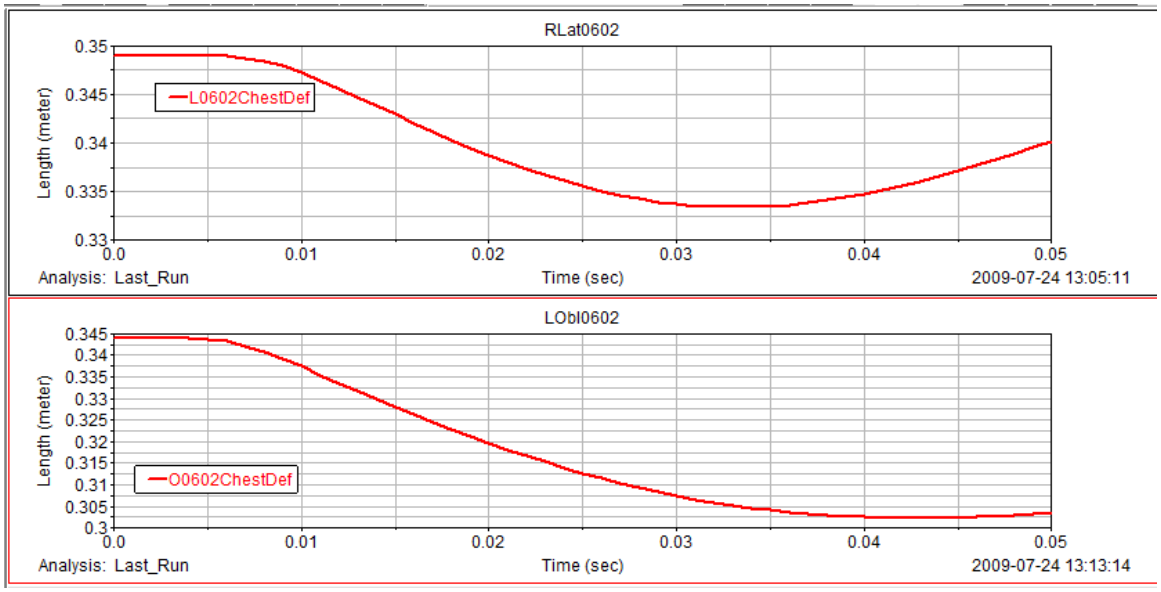
RLat0602
L0602ChestDef
Length (meter)
0.35
0.345
0.34
0.335
0.33
0.0
0.01
0.02
0.03
0.04
0.05
Analysis: Last_Run
Time (sec)
2009-07-24 13:05:11
LObl0602
O0602ChestDef
Length (meter)
0.345
0.34
0.335
0.33
0.325
0.32
0.315
0.31
0.305
0.3
0.0
0.01
0.02
0.03
0.04
0.05
Analysis: Last_Run
Time (sec)
2009-07-24 13:13:14

APPENDIX B— SimMechanics Model of Thoracic Deflection

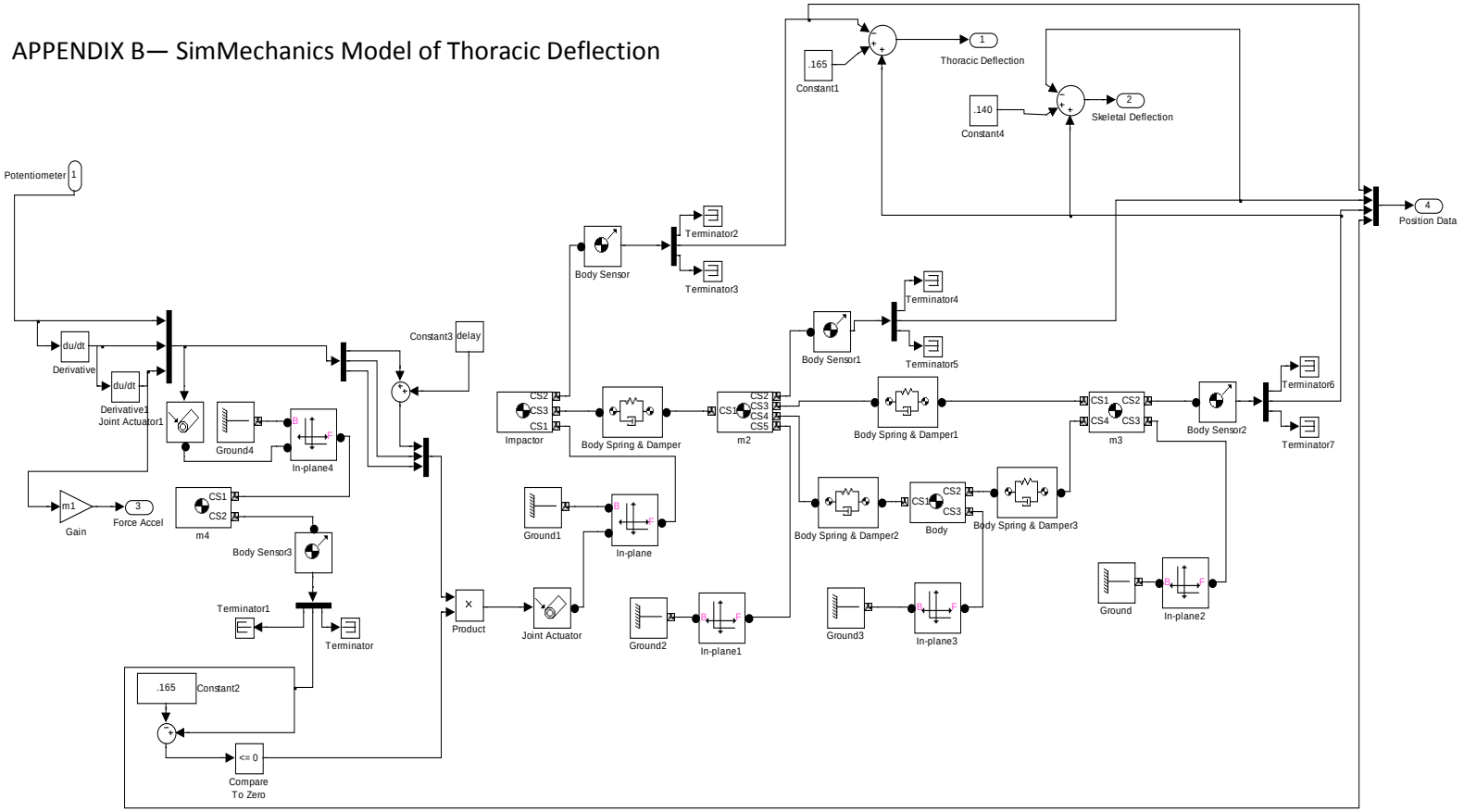

APPENDIX C—Simulation and Optimization Matlab Code

Low Speed Matlab Simulation Code—

```
function [SimTDLatLS,SimSDLatLS,
SimIFLatLS,ExpTDLatLS,ExpIFALatLS,YLat,Time]=LateralLowSpeedManD2(ThorMass,Mo
delInputs,n)

%Defining Inputs:
%n=Number of Desired Data Points
%Ram Accel=Array of Ram Impactor Accelerometer Data with
%   RamAccel(:,1)=Time and
%   RamAccel(:,2)=Accel Data
%ThorMass=Average Effective Mass of the Thorax for Appropriate Thoracic
%   Impact Direction
%ModelInputs=Array Defining Model Parameters
%   ModelInputs(1)=Effective Mass of Elements (m2)
%   ModelInputs(2)=Stiffness of Ribs (k23)
%   ModelInputs(3)=Damping of Diaphragm-Comp (c23c)
%   ModelInputs(4)=Viscoelastic Spring Stiffness (kv23)
%   ModelInputs(5)=Viscoelastic Damping Stiffness (cv23)
%   ModelInputs(6)=Gap Between Ram and Thorax at Time Zero (delay)
%Note:Need to Define Global Variables in Workspace Prior to Running
%Function

%Defining Global Variables (ie Model Inputs)------------------------------

global m1
global m2
global m3
global k12
global k23
global c23
global kv23
global cv23
global delay

%Calculating Model Parameters-------------------------------------------------

m1=24.82;
m2=ModelInputs(1);
m3=ThorMass-2*m2;
k12=132000;
k23=ModelInputs(2);
c23=ModelInputs(3);
kv23=ModelInputs(4);
cv23=ModelInputs(5);
delay=ModelInputs(6);

%Importing Experimental Data--------------------------------------------------

ExpData=load('AVGLAT.mat');
RamAccel=load('AVGLATAccF.mat');
RamPot=load('AVGLATPot.mat');
```

```
%Running Simulink Model-------------------------------------------------------

options=simset('SaveFormat','Structure');
timespan=[0 .06];

input=[RamPot.AVGLATPot(:,1) .01*RamPot.AVGLATPot(:,2)];

[T,X,ChestDef,SkelDef,ImpactForceP,
Ysim]=sim('UniversalManDelay',timespan,options,input);  %Modified

%Resampling Data---------------------------------------------------------------

%Simulated--

Time=linspace(0,.06,n);
SimTDLatLS=interp1(T, 1000*ChestDef.signals.values,Time);
SimSDLatLS=interp1(T, 1000*SkelDef.signals.values,Time);  %Modified
SimIFLatLS=interp1(linspace(0,.06,length(RamAccel.AVGLATAccF(50:1259,2))),
m1*9.806*RamAccel.AVGLATAccF(50:1259,2),Time);
YLat(1:n,1)=interp1(T, Ysim.signals.values(:,1),Time);
YLat(1:n,2)=interp1(T, Ysim.signals.values(:,2),Time);
YLat(1:n,3)=interp1(T, Ysim.signals.values(:,3),Time);
YLat(1:n,4)=interp1(T, Ysim.signals.values(:,4),Time);

%Experimental--

ExpDefShort=ExpData.AVGLAT(51:1221,2); %Need to readjust boundaries if
timespan ever changes
ExpForceShort=ExpData.AVGLAT(51:1221,3); %Need ot readjust boundaries if
timespan ever changes
ExpForceShortA=9.8*m1*RamAccel.AVGLATAccF(50:1259,2); %Need to readjust if
timespan ever changes

ExpTDLatLS=interp1(linspace(0,.06,length(ExpDefShort)), ExpDefShort,Time);
ExpIFALatLS=interp1(linspace(0,.06,length(ExpForceShortA)),
ExpForceShortA,Time);
```

Low Speed Oblique Matlab Simulation Code—

```
function [SimTDOblLS,SimSDOblLS,
SimIFOblLS,ExpTDOblLS,ExpIFAOblLS,YObl,Time]=ObliqueLowSpeedManD2(ThorMass,Mo
delInputs,n)

%Defining Inputs:
%n=Number of Desired Data Points
%Ram Accel=Array of Ram Impactor Accelerometer Data with
%   RamAccel(:,1)=Time and
%   RamAccel(:,2)=Accel Data
%ThorMass=Average Effective Mass of the Thorax for Appropriate Thoracic
%   Impact Direction
%ModelInputs=Array Defining Model Parameters
%   ModelInputs(1)=Effective Mass of Elements (m2)
%   ModelInputs(2)=Stiffness of Ribs (k23)
```

```
%   ModelInputs(3)=Damping of Diaphragm-Comp (c23c)
%   ModelInputs(4)=Viscoelastic Spring Stiffness (kv23)
%   ModelInputs(5)=Viscoelastic Damping Stiffness (cv23)
%   ModelInputs(6)=Gap Between Ram and Thorax at Time Zero (delay)
%Note:Need to Define Global Variables in Workspace Prior to Running
%Function

%Defining Global Variables (ie Model Inputs)------------------------------

global m1
global m2
global m3
global k12
global k23
global c23
global kv23
global cv23
global delay

%Calculating Model Parameters---------------------------------------------

m1=24.82;
m2=ModelInputs(1);
m3=ThorMass-2*m2;
k12=132000;
k23=ModelInputs(2);
c23=ModelInputs(3);
kv23=ModelInputs(4);
cv23=ModelInputs(5);
delay=ModelInputs(6);

%Importing Experimental Data----------------------------------------------

ExpData=load('AVGOBL.mat');
RamAccel=load('AVGOBLAccF.mat');
RamPot=load('AVGOBLPot.mat');

%Running Simulink Model---------------------------------------------------

options=simset('SaveFormat','Structure');
timespan=[0 .06];

input=[RamPot.AVGOBLPot(:,1) .01*RamPot.AVGOBLPot(:,2)];

[T,X,ChestDef, SkelDef, ImpactForceP,
Ysim]=sim('UniversalManDelay',timespan,options,input);

%Resampling Data----------------------------------------------------------

%Simulated--

Time=linspace(0,.06,n);
SimTDOblLS=interp1(T, 1000*ChestDef.signals.values,Time);
SimSDOblLS=interp1(T, 1000*SkelDef.signals.values, Time);
```

```
SimIFOblLS=interp1(linspace(0,.06,length(RamAccel.AVGOBLAccF(50:1259,2))),
m1*9.806*RamAccel.AVGOBLAccF(50:1259,2),Time);
YObl(1:n,1)=interp1(T, Ysim.signals.values(:,1),Time);
YObl(1:n,2)=interp1(T, Ysim.signals.values(:,2),Time);
YObl(1:n,3)=interp1(T, Ysim.signals.values(:,3),Time);
YObl(1:n,4)=interp1(T, Ysim.signals.values(:,4),Time);

%Experimental--

ExpDefShort=ExpData.AVGOBL(51:1221,2); %Need to readjust boundaries if
timespan ever changes
ExpForceShort=ExpData.AVGOBL(51:1221,3); %Need ot readjust boundaries if
timespan ever changes
ExpForceShortA=9.8*m1*RamAccel.AVGOBLAccF(50:1259,2); %Need to readjust if
timespan ever changes

ExpTDOblLS=interp1(linspace(0,.06,length(ExpDefShort)), ExpDefShort,Time);
ExpIFAOblLS=interp1(linspace(0,.06,length(ExpForceShortA)),
ExpForceShortA,Time);
```

High Speed Lateral Matlab Simulation Code—

```
function
[SimTDLatLS,SimIFLatLS,ExpTDLatLS,ExpIFLatLS,ExpIFALatLS,YLat,Time]=LateralLo
wSpeedManD2HS(ThorMass,ModelInputs,n)

%Defining Inputs:
%n=Number of Desired Data Points
%Ram Accel=Array of Ram Impactor Accelerometer Data with
%   RamAccel(:,1)=Time and
%   RamAccel(:,2)=Accel Data
%ThorMass=Average Effective Mass of the Thorax for Appropriate Thoracic
%   Impact Direction
%ModelInputs=Array Defining Model Parameters
%   ModelInputs(1)=Effective Mass of Elements (m2)
%   ModelInputs(2)=Stiffness of Ribs (k23)
%   ModelInputs(3)=Damping of Diaphragm-Comp (c23c)
%   ModelInputs(4)=Viscoelastic Spring Stiffness (kv23)
%   ModelInputs(5)=Viscoelastic Damping Stiffness (cv23)
%   ModelInputs(6)=Gap Between Ram and Thorax at Time Zero (delay)
%Note:Need to Define Global Variables in Workspace Prior to Running
%Function

%Defining Global Variables (ie Model Inputs)------------------------------

global m1
global m2
global m3
global k12
global k23
global c23
global kv23
global cv23
global delay
```

```
%Calculating Model Parameters-----------------------------------------------

m1=24.82;
m2=ModelInputs(1);
m3=ThorMass-2*m2;
k12=132000;
k23=ModelInputs(2);
c23=ModelInputs(3);
kv23=ModelInputs(4);
cv23=ModelInputs(5);
delay=ModelInputs(6);

%Importing Experimental Data-------------------------------------------------

ExpData=load('AVGLATHS.mat');
RamAccel=load('AVGLATAccFHS.mat');
RamPot=load('AVGLATPotHS.mat');

%Running Simulink Model------------------------------------------------------

options=simset('SaveFormat','Structure');
timespan=[0 .05];

input=[RamPot.AVGLATPotHS(:,1) .01*RamPot.AVGLATPotHS(:,2)];
[T,X,ChestDef,SkelDef, ImpactForceP,
Ysim]=sim('UniversalManDelay',timespan,options,input); %Modified

%Resampling Data-------------------------------------------------------------

Time=linspace(0,.06,n);
SimTDLatLS=interp1(T, 1000*ChestDef.signals.values,Time);
SimSDLatLS=interp1(T, 1000*SkelDef.signals.values,Time);  %Modified
SimIFLatLS=interp1(linspace(0,.06,length(RamAccel.AVGLATAccFHS(:,2))),
m1*9.806*RamAccel.AVGLATAccFHS(:,2),Time);
YLat(1:n,1)=interp1(T, Ysim.signals.values(:,1),Time);
YLat(1:n,2)=interp1(T, Ysim.signals.values(:,2),Time);
YLat(1:n,3)=interp1(T, Ysim.signals.values(:,3),Time);
YLat(1:n,4)=interp1(T, Ysim.signals.values(:,4),Time);

%Experimental--

ExpDefShort=ExpData.AVGLATHS(51:1221,2); %Need to readjust boundaries if
timespan ever changes
ExpForceShort=ExpData.AVGLATHS(51:1221,3); %Need ot readjust boundaries if
timespan ever changes
ExpForceShortA=9.8*m1*RamAccel.AVGLATAccFHS(50:1259,2); %Need to readjust if
timespan ever changes

ExpTDLatLS=interp1(linspace(0,.06,length(ExpDefShort)), ExpDefShort,Time);
ExpIFLatLS=interp1(linspace(0,.06,length(ExpForceShort)),
ExpForceShort,Time);
ExpIFALatLS=interp1(linspace(0,.06,length(ExpForceShortA)),
ExpForceShortA,Time);
```

High Speed Oblique Simulation Code—

```
function
[SimTDOblLS,SimIFOblLS,ExpTDOblLS,ExpIFOblLS,ExpIFAOblLS,YObl,Time]=ObliqueLo
wSpeedManD2HS(ThorMass,ModelInputs,n)

%Defining Inputs:
%n=Number of Desired Data Points
%Ram Accel=Array of Ram Impactor Accelerometer Data with
%   RamAccel(:,1)=Time and
%   RamAccel(:,2)=Accel Data
%ThorMass=Average Effective Mass of the Thorax for Appropriate Thoracic
%   Impact Direction
%ModelInputs=Array Defining Model Parameters
%   ModelInputs(1)=Effective Mass of Elements (m2)
%   ModelInputs(2)=Stiffness of Ribs (k23)
%   ModelInputs(3)=Damping of Diaphragm-Comp (c23c)
%   ModelInputs(4)=Viscoelastic Spring Stiffness (kv23)
%   ModelInputs(5)=Viscoelastic Damping Stiffness (cv23)
%   ModelInputs(6)=Gap Between Ram and Thorax at Time Zero (delay)
%Note:Need to Define Global Variables in Workspace Prior to Running
%Function

%Defining Global Variables (ie Model Inputs)------------------------------

global m1
global m2
global m3
global k12
global k23
global c23
global kv23
global cv23
global delay

%Calculating Model Parameters---------------------------------------------

m1=24.82;
m2=ModelInputs(1);
m3=ThorMass-2*m2;
k12=132000;
k23=ModelInputs(2);
c23=ModelInputs(3);
kv23=ModelInputs(4);
cv23=ModelInputs(5);
delay=ModelInputs(6);

%Importing Experimental Data----------------------------------------------

ExpData=load('AVGOBLHS.mat');
RamAccel=load('AVGOBLAccFHS.mat');
RamPot=load('AVGOBLPotHS.mat');

%Running Simulink Model---------------------------------------------------
```

```
options=simset('SaveFormat','Structure');
timespan=[0 .05];

input=[RamPot.AVGOBLPotHS(:,1) .01*RamPot.AVGOBLPotHS(:,2)];

[T,X,ChestDef,SkelDef, ImpactForceP,
Ysim]=sim('UniversalManDelay',timespan,options,input); %Modified

%Resampling Data-------------------------------------------------------------

Time=linspace(0,.06,n);
SimTDOblLS=interp1(T, 1000*ChestDef.signals.values,Time);
SimSDOblLS=interp1(T, 1000*SkelDef.signals.values, Time);
SimIFOblLS=interp1(linspace(0,.06,length(RamAccel.AVGOBLAccFHS(:,2))),
m1*9.806*RamAccel.AVGOBLAccFHS(:,2),Time);
YObl(1:n,1)=interp1(T, Ysim.signals.values(:,1),Time);
YObl(1:n,2)=interp1(T, Ysim.signals.values(:,2),Time);
YObl(1:n,3)=interp1(T, Ysim.signals.values(:,3),Time);
YObl(1:n,4)=interp1(T, Ysim.signals.values(:,4),Time);

%Experimental--

ExpDefShort=ExpData.AVGOBLHS(51:1221,2); %Need to readjust boundaries if
timespan ever changes
ExpForceShort=ExpData.AVGOBLHS(51:1221,3); %Need ot readjust boundaries if
timespan ever changes
ExpForceShortA=9.8*m1*RamAccel.AVGOBLAccFHS(50:1259,2); %Need to readjust if
timespan ever changes

ExpTDOblLS=interp1(linspace(0,.06,length(ExpDefShort)), ExpDefShort,Time);
ExpIFOblLS=interp1(linspace(0,.06,length(ExpForceShort)),
ExpForceShort,Time);
ExpIFAOblLS=interp1(linspace(0,.06,length(ExpForceShortA)),
ExpForceShortA,Time);
```

Optimization Scheme 1 Code—

```
function F=RunOptLatDual(x2,xData)

Time=xData; %#ok<NASGU>

[SLatDef, SLatSDef, SLatForce, ELatDef, ELatForceA, YLat,
Time]=LateralLowSpeedManD2(28.11,x2,600);
[SLatDefHS, SLatForceHS, ELatDefHS, ELatForceIHS, ELatForceAHS, YLatHS,
TimeHS]=LateralLowSpeedManD2HS(36.90,x2,500);

figure(1)
plot(Time,SLatDef,'r',Time,ELatDef,'g',TimeHS,SLatDefHS,'r',TimeHS,ELatDefHS,
'g')
title('Current Error between Experimental and Simulated Thoracic Deflection')
xlabel('Time [sec]'); ylabel('Error [mm]')
```

```
global xnow
global count

format bank
format compact

disp('1 Completed Iteration-----------------------------------------------')

xnow= x2;
disp(xnow)

disp('Count-----')
count=count+1;
disp(count)

F=[SLatDef'; SLatDefHS'];
```

Optimization Scheme 2 Code—

```
function F=RunOptLowSpeedDual(x2,xData)

Time=xData; %#ok<NASGU>

[SLatDef, SLatSDef, SLatForce, ELatDef, ELatForceA, YLat,
Time]=LateralLowSpeedManD2(28.11,x2,600);

[SOblDef, SOblSDef, SOblForce, EOblDef, EOblForceA, YObl,
Time]=ObliqueLowSpeedManD2(29.28,x2,600);

figure(1)
plot(Time,SLatDef,'r',Time,ELatDef,'g',Time,SOblDef,'r',Time,EOblDef,'g')
title('Current Error between Experimental and Simulated Thoracic Deflection')
xlabel('Time [sec]'); ylabel('Error [mm]')

global xnow
global count

format bank
format compact

disp('1 Completed Iteration-----------------------------------------------')

xnow= x2;
disp(xnow)

disp('Count-----')
count=count+1;
disp(count)

F=[SLatDef'; SOblDef'];
```

Appendix D—Averaged Input/Output Experimental Data used in Modeling for Each Experimental Group

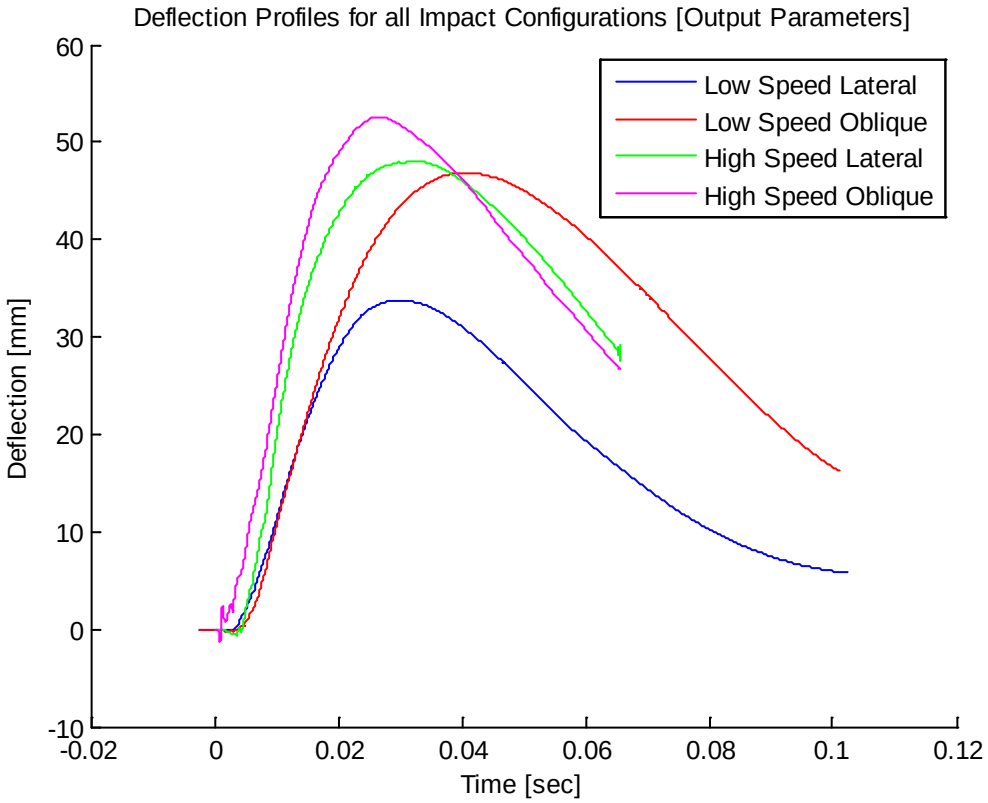

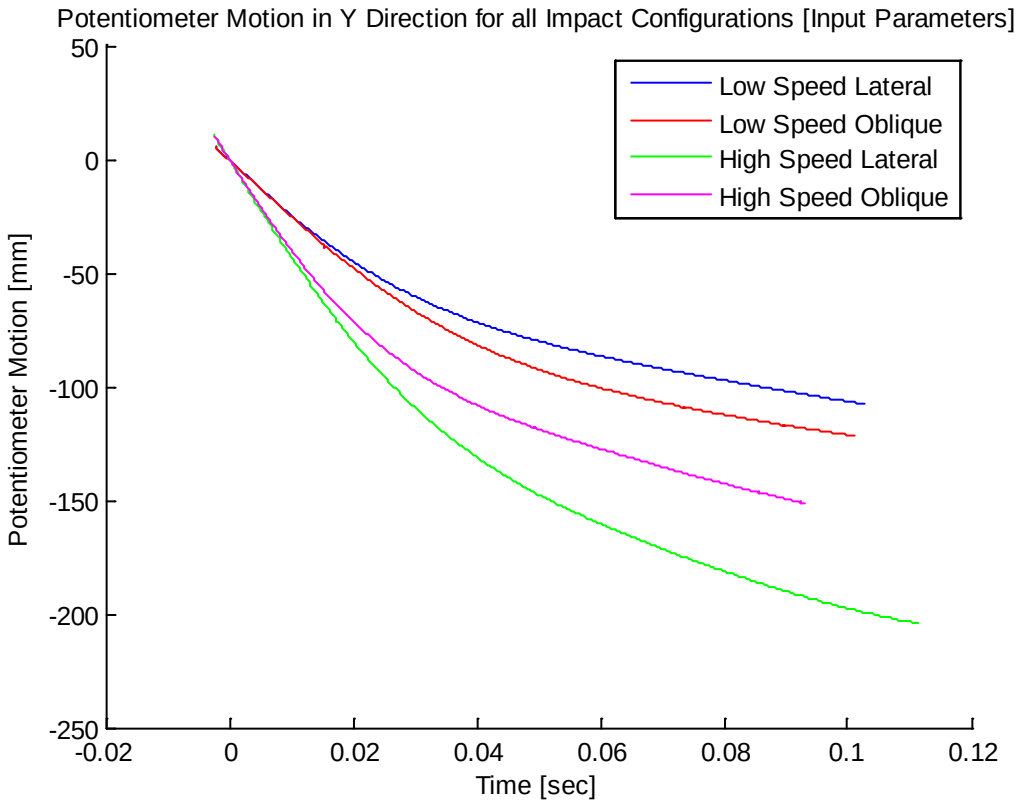
Potentiometer Motion in Y Direction for all Impact Configurations [Input Parameters]
Low Speed Lateral
Low Speed Oblique
High Speed Lateral
High Speed Oblique
Potentiometer Motion [mm]
Time [sec]
50
0
-50
-100
-150
-200
-250
-0.02
0
0.02
0.04
0.06
0.08
0.1
0.12